FEDERAL UNIVERSITY OF SANTA CATARINA
JOINVILLE TECHNOLOGICAL CENTER
MECHATRONIC ENGINEERING

MARIA LUIZA FONTES DANTAS

PRECISION AUTOMATION OF A MICROLENS OPTICAL ALIGNMENT PROCESS USING AN AUTOCOLLIMATOR

Joinville
2024

MARIA LUIZA FONTES DANTAS

PRECISION AUTOMATION OF A MICROLENS OPTICAL ALIGNMENT PROCESS USING AN AUTOCOLLIMATOR

This graduation thesis is presented to fulfill the partial requirement to obtain the title of bachelor in the course of Mechatronic Engineering, at the Joinville Technology Center, from the Federal University of Santa Catarina.

Advisor: Dr. Alexandro Garro Brito

Co-advisor: Christian Batzel

Joinville
2024

Dedico este trabalho aos meus pais, Jacqueline e Hermano, por todo o apoio incondicional, pela torcida em cada etapa da minha jornada e por acreditarem em mim em tudo o que me propus a realizar.

ACKNOWLEDGMENTS

First and foremost, I would like to thank my family, especially my mother Jacqueline and my father Hermano, for their unconditional support and for always believing in me, even during moments when I doubted myself. Everything I achieve in life will always be our achievement.

I would also like to extend my gratitude to my assistants at the Fraunhofer Institute of Production Technology: Nils Hillmer, Burhan Berk Kurhan, and especially Christian Batzel, who guided me and provided invaluable insights throughout the development of this project.

My thanks also go to my colleagues at IPT, who made my stay in Germany both enjoyable and enriching. Moving to an unfamiliar country could have been a lonely experience, but you made this period truly special.

Finally, I am deeply grateful to the friends I made during my undergraduate studies in Joinville. Moving to the other side of the country was a significant challenge, but with you, I found a second family. Thank you for staying present, even from afar, while I was in Germany.

“ In the middle of every difficulty lies opportunity. ”

Albert Einstein

RESUMO

Este trabalho propõe e avalia um método para a automatização do processo de construção de microlentes destinadas a endoscópios descartáveis. A motivação principal é reduzir o risco de contaminação cruzada associado ao uso de endoscópios reutilizáveis, mesmo após processos de limpeza. Para viabilizar a produção de componentes descartáveis, é necessário explorar materiais de baixo custo, que apresentam propriedades ópticas inferiores. Assim, é crucial implementar um processo de montagem preciso para compensar as limitações dos materiais e assegurar um desempenho óptico satisfatório. A automatização do processo surge como uma solução eficiente, permitindo maior rapidez, redução de custos e precisão na montagem. Neste contexto, o autocolimador, por sua capacidade de manipulação e análise de lentes de tamanho reduzido, foi utilizado como ferramenta principal. O trabalho tem como objetivo principal avaliar a eficácia do método proposto, identificando erros e investigando possíveis melhorias no processo. Os resultados obtidos demonstraram que o método foi capaz de realizar o posicionamento das peças com precisão satisfatória, embora ainda existam margens para aprimoramentos futuros. As melhorias implementadas ao longo do estudo contribuíram para a evolução do processo, que apresentou resultados promissores na automatização da construção de microlentes para aplicações em endoscópios com partes descartáveis.

Palavra-chave: Autocolimador. Micro lentes. Automação de precisão.

ABSTRACT

This work proposes and evaluates a method for automating the construction process of microlenses intended for disposable endoscopes. The main motivation is to reduce the risk of cross-contamination associated with reusable endoscopes, even after cleaning procedures. To enable the production of disposable components, it is necessary to explore low-cost materials, which typically have inferior optical properties. Therefore, implementing a precise assembly process is crucial to compensate for these material limitations and ensure satisfactory optical performance. Process automation emerges as an efficient solution, enabling faster, more cost-effective assembly while maintaining satisfactory precision. In this context, the autocollimator was employed as the primary tool due to its capability to handle and analyze small lenses. The main objective of this study is to evaluate the effectiveness of the proposed method, identifying errors and exploring potential improvements in the process. The results demonstrated that the method successfully positioned the components with satisfactory accuracy, although there is still room for future refinements. The improvements implemented during the study contributed to the evolution of the process, which showed promising results in automating the construction of microlenses for use in disposable endoscopes.

Keywords: Autocollimator. Microlenses. Precision automation.

LIST OF FIGURES

LIST OF TABLES

SUMÁRIO

1 INTRODUCTION

With the advancement of technology, it has become possible to produce technological devices with reduced size and increased processing power, such as mobile phones. The development of techniques capable of reducing the size of components is essential for expanding their range of applications and paving the way for their overall improvement. Generally, the steady increase in processing speed can be attributed to this trend (KEYES, 1972). One of the devices included in this process is the camera, where significant efforts have been made to minimize lens size without compromising quality.

The production of microlenses has significantly increased in recent years. This growth is driven by the rising demand from applications such as micro-cameras used in mobile phones and endoscopes. An endoscope is an instrument used in endoscopy, a technique that allows for the inspection, manipulation, and treatment of internal organs within the human body using micro-cameras, without the need for large incisions (GROEN, 2017). This method has replaced open surgeries, offering substantial benefits such as smaller scars, lower fatality rates, and faster recovery times (GAAB, 2013).

The use of endoscopes presents significant challenges related to their cleaning and decontamination. These devices, used in the exploration of internal cavities within the human body, are highly susceptible to contamination. This can result in serious complications when the equipment is reused on other patients. Although rigorous decontamination procedures are performed after each use, the literature has documented cases of infections associated with bacteria, viruses, fungi, and helminths (MARTINY et al., 2004).

A potential solution to this problem is the use of disposable components in endoscopes, which could be replaced between procedures. However, this approach presents practical challenges, such as the high cost associated with the frequent disposal of parts and the increased manufacturing time for endoscopes, given that many of the components are small and complex to construct. To mitigate these challenges, it is proposed to replace the camera lens material in the endoscope with plastic, which would reduce costs. However, plastic lenses do not possess optical properties as advanced as glass lenses, necessitating highly precise manufacturing to preserve image quality. The margin of error in the construction of plastic lenses must be minimal to ensure that visual quality is not significantly compromised.

Given the continuous advancement in the miniaturization of technological structures, it has become necessary to develop new construction methods and quality control processes that keep pace with the reduction in structural dimensions and material

changes, without compromising image resolution. In this context, the present work proposes and conducts a detailed analysis of a method for constructing a plastic lens system, specifically designed for use in an endoscope camera. The proposed structure consists of three lenses and an iris, with their configurations and arrangement shown in Figure 1.

Figure 1 – Lens System.

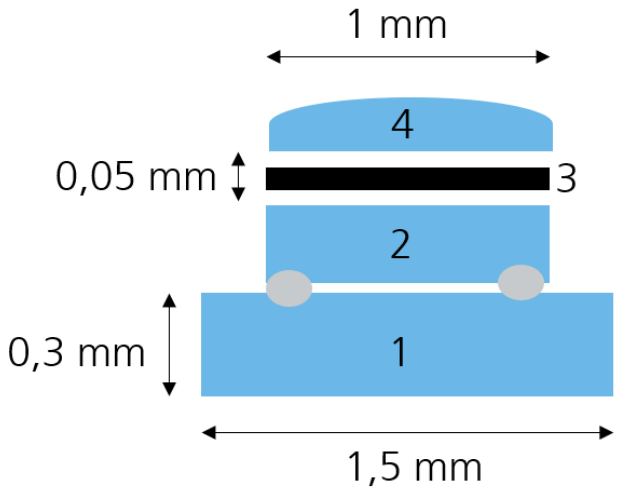

Source: Author (2024).

The production of optical systems, especially those that use multiple lenses, requires a high degree of precision to function correctly (LANGEHANENBERG et al., 2011). In addition to errors caused by the lens manufacturing process itself, such as inaccuracies in its shape or optical properties, failures in the positioning of any of the multiple lenses can also lead to significant degradation in camera quality. When dealing with the production of microlenses, these issues are exacerbated, necessitating the use of more complex and demanding techniques.

One solution for dealing with the reduced size of structures is to use an autocollimator to acquire the necessary data. Autocollimators are versatile optical devices widely used for precise, non-contact measurements of angles on reflective surfaces, they are applicable in various areas of metrology and industry, such as the adjustment of angles, straightness, parallelism, and perpendicularity of machine tools (GECKELER; JUST, 2018). Additionally, these devices have proven to be highly accurate in angular metrology, especially in measuring complex shapes on optical surfaces.

The work is organized into the following sections: theoretical foundation, methodology, data presentation and analysis, improvements, and conclusion. The theoretical foundation presents the foundational texts that support the development of the study, providing the necessary basis for understanding the concepts involved. The methodology details the process developed, including the materials and methods employed to

achieve the proposed objectives. The data presentation and analysis section displays the results obtained throughout the process, accompanied by a critical evaluation of their performance and impact. The improvements section addresses suggestions and implementations of enhancements identified from the data analysis, presenting the results of these changes and their corresponding evaluation. Finally, the conclusion summarizes the overall findings of the work, discussing whether the initially proposed objectives were achieved and highlighting the study's contributions.

1.1 OBJECTIVES

To address the challenge of automating the construction of microlens systems for use in endoscope cameras, the following objectives are proposed:

1.1.1 General Objective

This work aims to explore a method for constructing optical lens systems, assess its effectiveness in automating the construction process, and evaluate whether the results achieved meet the required precision standards.

1.1.2 Specific Objectives

The specific objectives of this work are:

- Assess the ability of the autocollimator in obtaining suitable images for acquiring the data necessary for automating the construction process;
- Develop a code for the automatic acquisition of relevant data for the process;
- Develop a code that analyzes the collected data and ensures the correct positioning of the lenses;
- Test the precision and effectiveness of the lens positioning, and verify whether the results are satisfactory.

2 THEORETICAL FOUNDATION

In this chapter, the theoretical foundation used to produce the entire work will be discussed, divided into the key pillars of the autocollimator, centering measurement techniques and machine vision.

The production of optical systems, particularly those utilizing multiple lenses, critically requires precision to ensure the proper functioning of the devices. Inaccuracies in lens manufacturing, such as variations in shape and optical properties of the material, as well as misalignment of the lenses, can significantly compromise the final quality of the system. These challenges are even more pronounced in systems that employ microlenses, thus requiring the adoption of more sophisticated and demanding techniques.

In this context, the automation of the optical system assembly process emerges as a promising solution to mitigate these issues. The use of precise measurement equipment, such as the autocollimator, is essential for acquiring reliable data, as well as the use of apropiate measuring technique and a well structured machine vision. Furthermore, the use of a high-precision actuator is critical for ensuring the exact positioning of the lenses during system assembly. Automating this process through a code developed to minimize errors is crucial to ensuring that the lens alignment is performed accurately, thereby validating the effectiveness of the proposed method and the quality of the produced optical system.

2.1 AUTOCOLLIMATOR

The autocollimator is a high-precision measuring instrument used to detect small angular displacements by combining the functionalities of collimators and telescopes.

2.1.1 Collimators

The collimator is an optical device that uses an objective lens combined with an illuminated reticle to align light beams. When light passes through the lens and the reticle, it emerges as parallel rays, resulting in the projection of the reticle's image at an apparently very distant position, referred to as infinity setting (TRIPTICS, 2013).

Changes in the position of the reticle relative to the lens's focal plane alter the shape of the emerging light beam, as illustrated in Figure 2. When the reticle is moved away from the lens, the beam becomes convergent, producing a real image of the reticle at a defined distance. Conversely, when the reticle is brought closer to the lens, the beam becomes divergent, creating a virtual image that, although situated at a finite

distance, still maintains the illusion of proximity. This latter configuration is referred to as finite distance setting (TRIPTICS, 2013).

Figure 2 – Different Configurations of a Collimator.

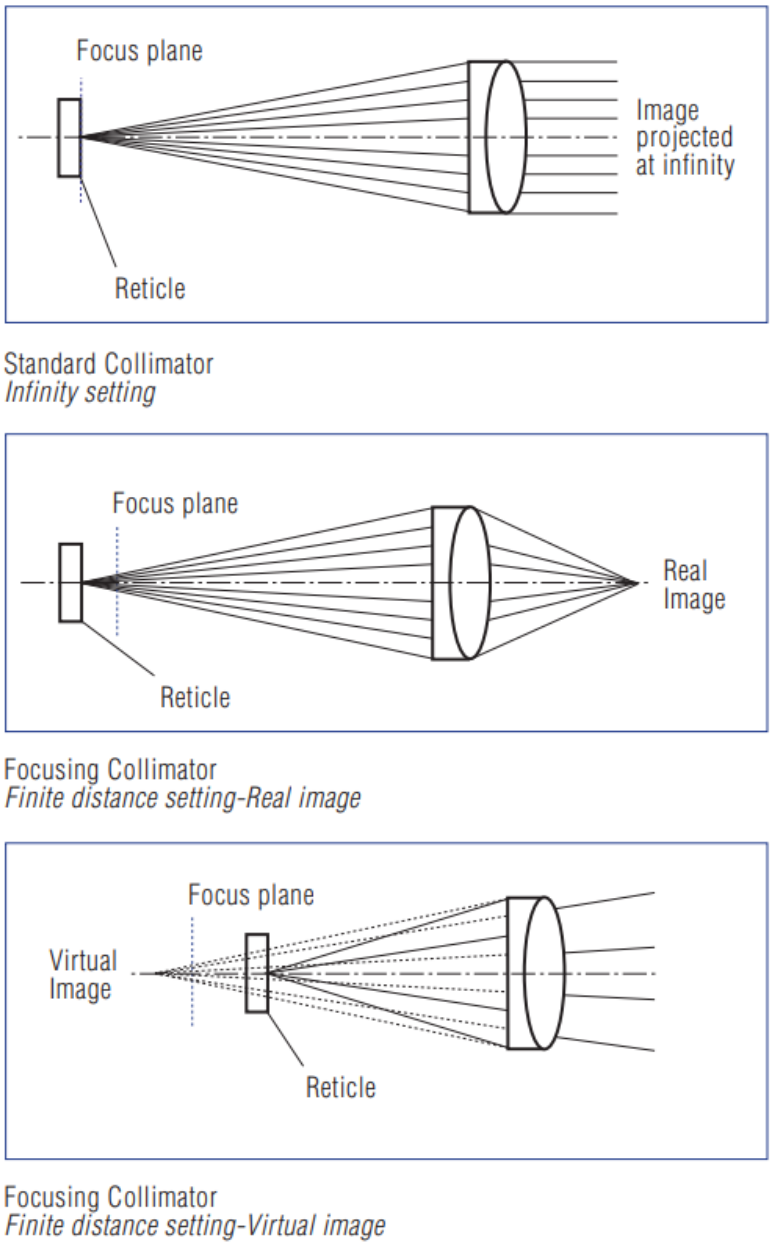

Source: (TRIPTICS, 2013).

This device is widely used in various optical instruments, such as telescopes and cameras, and is essential in applications requiring high precision, such as angular measurement equipment. In the case of its use in autocollimators, an adjustment for infinity is employed. This involves positioning the lens such that the light-emitting reticle is at its focal point, thereby collimating the rays emitted by it, as illustrated at the top of Figure 2.

2.1.2 Telescopes

A telescope operates by capturing and magnifying light from distant objects, allowing detailed observation of these objects. It enables the revelation of details that are imperceptible to the naked eye, making it an indispensable tool in fields such as astronomy and space exploration.

Figure 3 – Cassegrain Telescope.

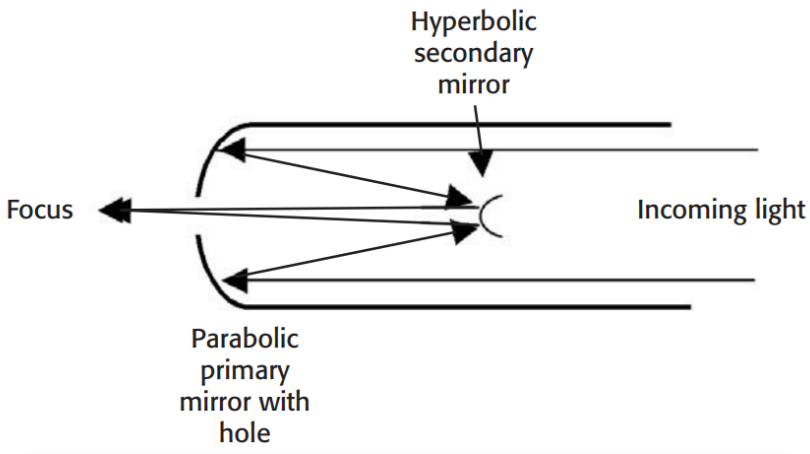

Source: (BALL, 2005).

The lens system within a telescope, or the assembly of lenses and mirrors, is crucial to the device's operation. The Cassegrain telescope, a model that serves as the basis for many modern devices and is illustrated in Figure 3, employs a parabolic primary mirror with a central aperture, this mirror directs light to a convex hyperbolic secondary mirror. The secondary mirror then reflects the light to a focal point located behind the primary mirror, thereby magnifying and focusing the image to make it observable (BALL, 2005).

2.1.3 Principle of Operation of an Autocollimator

The autocollimator combines the functions of collimators and telescopes. As illustrated in Figure 4, a collimator is used to project light into the system, while a telescope-like structure is employed to capture the image, allowing it to be magnified if necessary.

The autocollimator operates by emitting light that is directed via a beam splitter, which divides the beam into two distinct paths. One path directs the light to a capture area, where a camera is positioned to record the reflected image. The other path involves the light passing through an objective lens, which is precisely positioned so that the light source is at the lens's focal point, thereby ensuring that the light rays exit in a collimated manner. A simplified schematic of this configuration is illustrated in Figure 5.

Figure 4 – Basic Model of an Autocollimator.

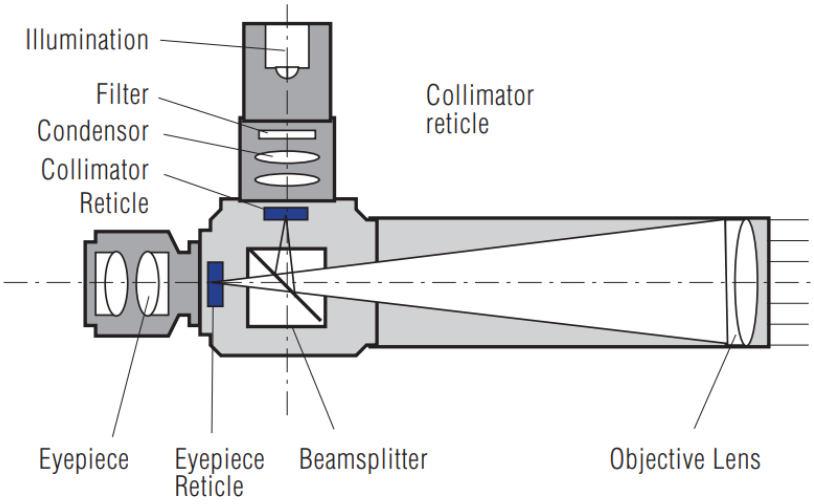

Source: (TRIPTICS, 2013).

The object under measurement must be positioned beyond the objective lens. A common application of the autocollimator, for example, is in assessing the flatness of a surface relative to the device. To perform this measurement, the light directly reaching the camera is compared with the light reflected from the surface, which is located beyond the objective lens. If the surface is perfectly flat, the image formed will be registered at the same point. Otherwise, the angle of inclination of the surface can be related to the distance between the position of the formed image and the original position.

Figure 5 – Simplified Model of an Autocollimator.

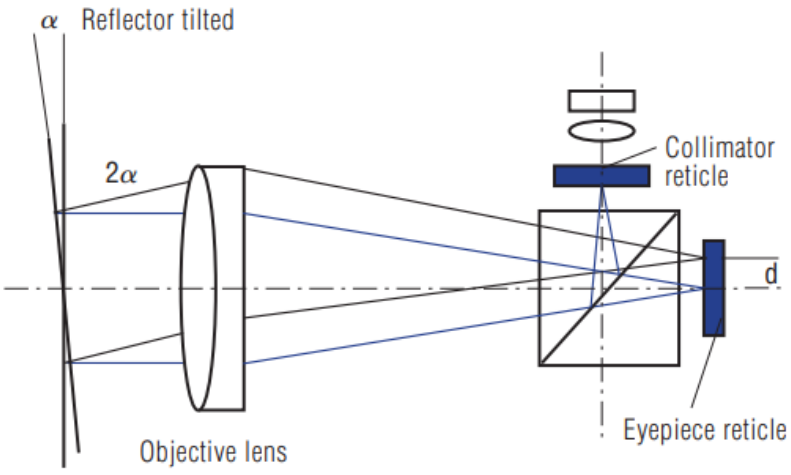

Source: (TRIPTICS, 2013).

2.2 CENTRALIZATION ERROR MEASUREMENT TECHNIQUE

Accurate assessment of true centering error is critical for ensuring the quality of optical systems, particularly in miniaturized designs. Therefore, it is essential to implement precise measurement techniques capable of detecting the tilt and tip of lenses relative to the intended reference axis.

To measure the centering error, an autocollimator that emits cross-shaped light is used, along with an optical setup that provides a wide focusing range. When the light strikes the lens of interest at a nearly perpendicular angle, part of it is reflected back. This reflection occurs when the autocollimator focuses the emitted light on the lens's center of curvature (HEINISCH et al., 2006). The cross image can then be observed on the camera attached to the autocollimator. It is important to note that if the lens is not perfectly aligned, the cross will be formed outside the reference axis, indicating a misalignment, as illustrated in Figure 6.

Figure 6 – Cross light on lens of interest.

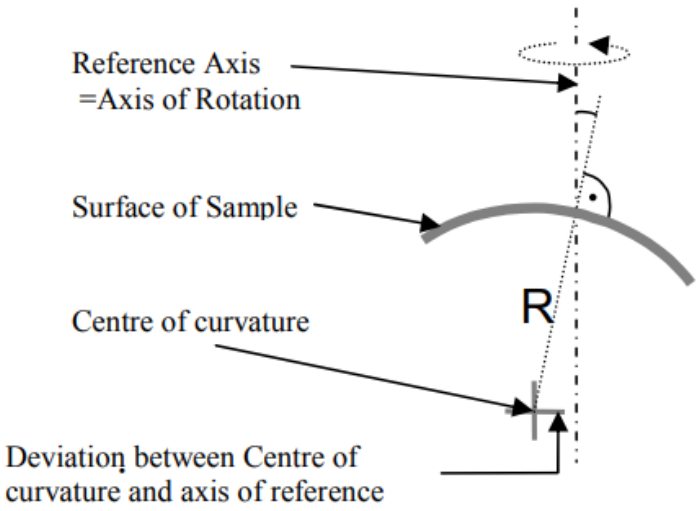

Source: (HEINISCH et al., 2006).

After obtaining the initial image of the lens of interest, it is necessary to assess whether its positioning is correct. To perform this evaluation, the lens can be rotated. If the lens is not perfectly aligned, the resulting image will display a circular pattern. The radius of the observed circle is directly proportional to the centering error of the lens, as illustrated in Figure 7.

The technique outlined previously is suitable for single surfaces; however, in practice, optical systems consist of multiple lenses. Therefore, it is necessary to measure each surface individually to determine its correct positioning. To achieve this, the light emitted by the autocollimator must be focused on a plane corresponding to

Figure 7 – Centering error captured by autocollimator camera.

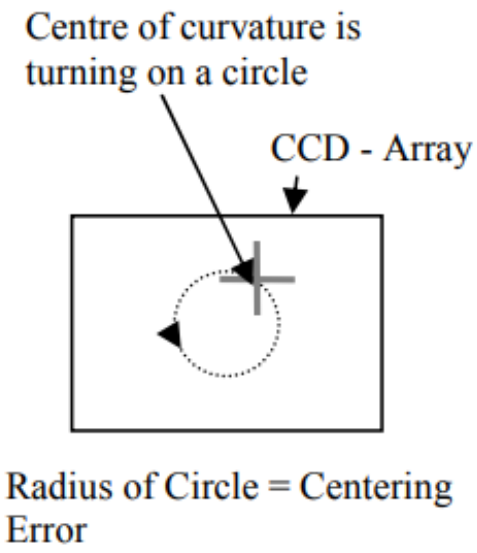

Source: (HEINISCH et al., 2006).

the center of curvature of the next spherical surface. This process can be challenging because, when obtaining the image of the second spherical surface, the light emitted by the autocollimator must pass through the first surface. This passage causes refraction, which must be taken into account during the calculations, as depicted in Figure 8. Consequently, the centering error of the first spherical surface impacts the calculation of the centering error for the second surface, and this effect propagates to subsequent surfaces (HEINISCH et al., 2006).

Figure 8 – Multiple surfaces.

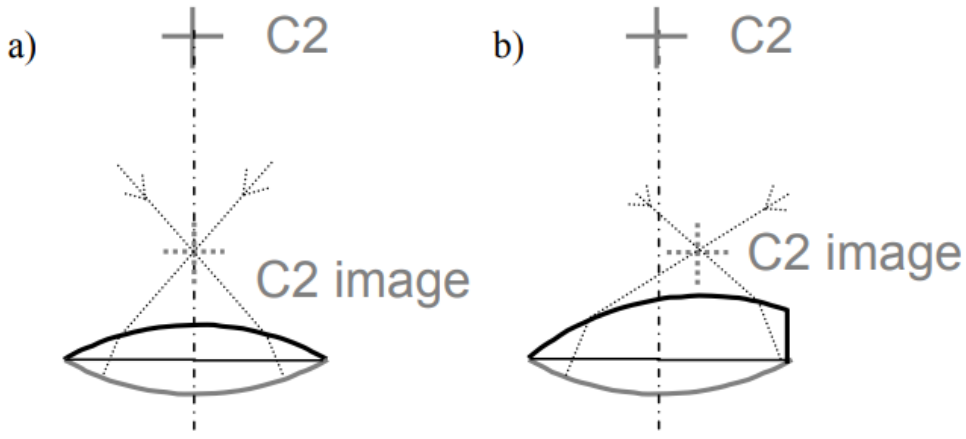

Source: (HEINISCH et al., 2006).

In the context of a lens system, such as those used in camera lenses, it is crucial to calculate the alignment for multiple lenses, each featuring two spherical surfaces. To determine the degree of inclination of each lens, the process of identifying the center of curvature for both spherical surfaces must be repeated for each side of the lens. A straight line can then be drawn between these points, establishing the lens axis. This procedure should be applied to all lenses within the system. By employing Cartesian coordinates, it is possible to construct a sample space representing the tilt axes of all lenses. Once the reference axis of the system is established, it is necessary to calculate the alignment error of each lens axis relative to the reference axis. A visual representation of the lens axes and the reference axis is illustrated in Figure 9.

Figure 9 – Lens axis and reference axis.

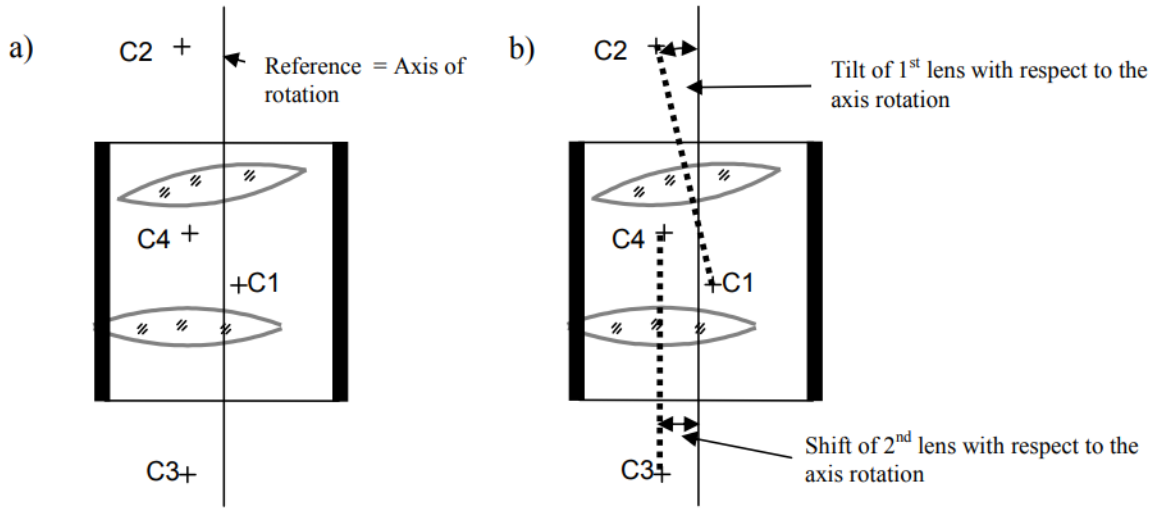

Source: (HEINISCH et al., 2006).

2.2.1 Aspherical Optics

The term "aspherical surface"refers to a surface that is rotationally symmetric but not spherical, meaning it has a variable radius of curvature (YUAN; LONG, 2003). Aspherical lenses are crucial components in reducing the size of optical systems, as they can be up to four times smaller than conventional lenses. Moreover, they reduce spherical aberrations, making them highly valuable in applications such as microcameras (KWEON; KIM, 2007). Although the radius of curvature of an aspherical lens is not constant, the previously reviewed technique for measuring tilt and alignment can still be applied. To achieve this, the center of curvature of the best-fitting sphere is determined, as illustrated in Figure 10

Figure 10 – Aspherical Lens.

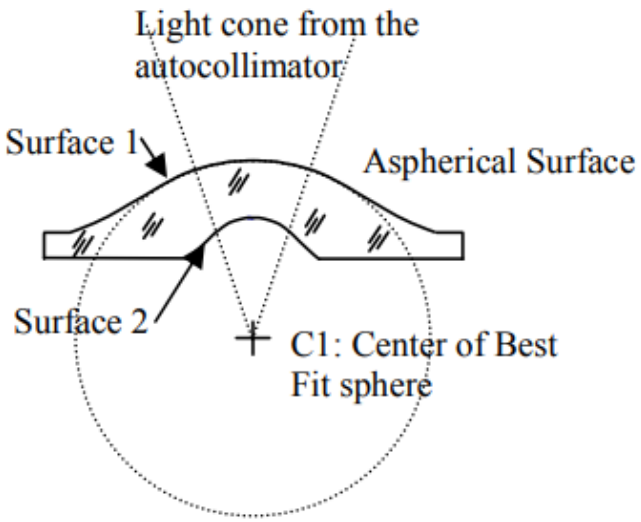

Source: (HEINISCH et al., 2006).

2.3 MACHINE VISION

The acquisition of essential data for accurate system analysis is a fundamental step in project development, and the field of Machine Vision plays a central role in this process. By utilizing sensors such as cameras, Machine Vision establishes an effective interface between the computer and the real world, enabling the capture and processing of visual data. In this context, tools like the autocollimator, combined with appropriate measurement techniques, allow for the acquisition of highly precise data, which can then be analyzed and used to achieve the specific objectives of the project.

The efficient operation of Machine Vision systems depends on several critical stages. The first phase involves image acquisition, where image sensors capture the visual data necessary for subsequent analysis. Following this, image processing is conducted, during which specific algorithms are applied to enhance image quality and extract the most relevant information. After processing, the next step is image analysis, where patterns are identified and objects are recognized, providing a detailed and accurate understanding of the captured visual content. These integrated stages are crucial to ensuring the system operates efficiently and meets the project's requirements.

2.3.1 Image Acquisition

Image acquisition is the initial step in machine vision systems and is essential for their proper functioning. The accuracy and effectiveness of subsequent analyses are inherently tied to the quality of the initial data; without adequate data, reliable analy-

ses cannot be performed. The primary goal of image acquisition is to convert an optical image (real-world data) into a numerical data array that can be processed and analyzed by a computer.

This process involves three main stages: first, an optical system is used to focus the incoming light energy; second, this energy is reflected by the object of interest; and finally, the capture of this energy is carried out by a sensor, which converts it into a digital format for further processing (MISHRA et al., 2017). This sequence is crucial to ensure that the visual data is properly translated into the computational environment and can be efficiently analyzed.

2.3.1.1 Ilumination

The energy utilized in image acquisition is light, making proper illumination essential for this process. Illumination plays a crucial role in enhancing the characteristics of the object with maximum contrast, addressing the challenge of improving the signal-to-noise ratio. The objective is to achieve homogeneous lighting with a consistent temporal and spatial distribution of brightness, or at least a predictable and contrasting distribution. This approach facilitates the application of image processing algorithms, rendering them simpler, more reliable, and stable.

Three important aspects to consider in image acquisition regarding illumination are contrast, exposure, and light direction. Contrast is a direct consequence of lighting and refers to the perception of light in relation to the average illumination of the image. When the brightest point of the image is significantly more illuminated than the darker areas, this difference results in a perception of high contrast. The contrast used for digital interpretation is calculated by the difference between the maximum and minimum gray values, as illustrated in Equation 1 (HORNBERG, 2017), where K_{dig} represents the contrast in images for digital interpretation, G_{max} is the maximum gray value, and G_{min} is the minimum gray value, which correspond to the brightest and darkest spots in the image, respectively. Adequate contrast enhances the accuracy of image processing algorithms and reduces the time required for processing.

$$K_{dig} = G_{max} - G_{min} \tag{1}$$

Exposure is a crucial parameter that establishes a connection between illumination, time, and camera hardware. Essentially, it refers to the amount of light allowed to enter the camera to generate the image, which is fundamental to the final quality of that image. An adequate amount of light must strike the sensor to ensure appropriate contrast; the image should neither be overexposed (excessively bright) nor underexposed (excessively dark). Exposure can be formally defined by Equation 2 (HORNBERG, 2017), where H represents exposure, E refers to the illumination of the object of interest, and t corresponds to the shutter time of the camera. The shutter time is the

duration for which the camera's shutter remains open to allow light to reach the sensor; a longer shutter time results in more light being captured, while a shorter time captures less light. Proper configuration of exposure is essential to ensure good contrast, leading to more efficient and precise image processing.

$$H = E \cdot t \tag{2}$$

A fundamental aspect of image acquisition in computer vision systems is the direction of light, which establishes the basis for the interaction of light with the object of interest. The direction of light can be classified into four main categories: diffuse, direct, telecentric, and structured (HORNBERG, 2017). Each of these modalities has specific characteristics that influence not only the quality of the resulting image but also the effectiveness of extracting relevant information about the analyzed object. The choice of lighting type should take into account the particularities of the application, as different methods can result in significant variations in the visual perception of the object.

Diffuse lighting is characterized by light that disperses in multiple directions, resulting in soft and even illumination on the object's surface. This configuration allows for the generation of soft shadows or even their absence, ensuring that the object is illuminated uniformly. Consequently, the color and brightness of the object remain relatively constant, which is particularly beneficial in situations requiring detailed analysis, as it minimizes the adverse effects of uneven lighting that could compromise the interpretation of the captured images (HORNBERG, 2017).

Direct lighting, on the other hand, involves light that travels in a straight line from the source to the surface without significant scattering. This approach is effective for highlighting edges and surface structures, creating bright highlights in areas where the light directly hits the surface. The presence of well-defined shadows resulting from this technique makes it ideal for applications that require high clarity in surface characteristics, such as quality inspections of materials and detection of visible defects (HORNBERG, 2017).

Telecentric lighting represents a special form of directed lighting, whose properties are obtained through a combination of an optical system and the light source, as seen in Figure 11 (HORNBERG, 2017). In this context, the light rays remain parallel, meaning that the light entering the system neither diverges nor converges, resulting in minimal perspective distortion. This characteristic makes telecentric lighting particularly suitable for applications that require precise measurements, such as industrial metrology and component inspection, allowing for consistent and reliable results.

Structured illumination, in turn, refers to a technique in which a pattern of light, such as grids, stripes, or dots, is projected onto a surface. The interaction of this pattern with the object can reveal important information about its shape, texture, and depth.

Figure 11 – Telecentric Lightning.

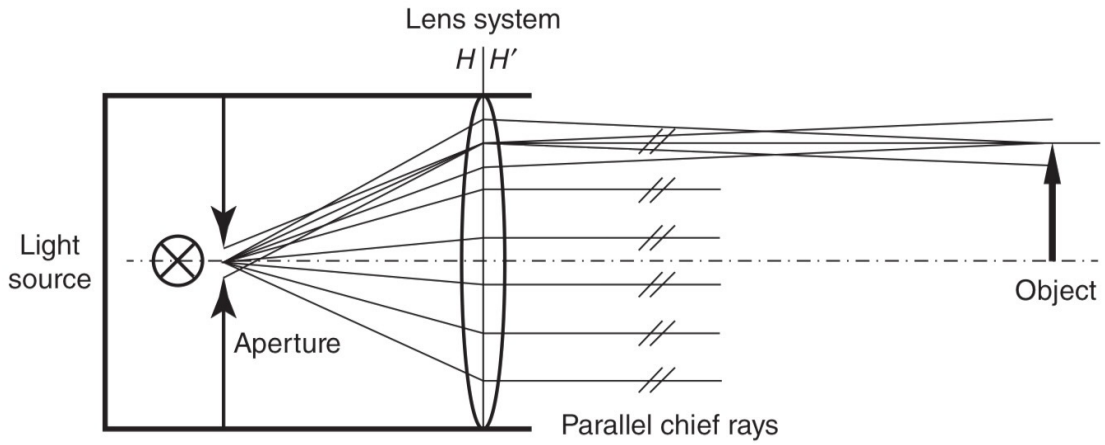

Source: (HORNBERG, 2017).

When observed through a camera, the deformation of the pattern can be analyzed to extract three-dimensional information or detect irregularities. This technique is valuable in applications that require 3D mapping and defect identification, providing a deeper understanding of the object's characteristics (HORNBERG, 2017).

In addition to previously discussed lighting techniques, front lighting and back lighting are two commonly employed methods in computer vision. Front lighting directs illumination onto the object's surface, typically aligned with the camera's axis, effectively highlighting surface characteristics such as colors and textures. However, this approach can create unwanted shadows or reduce contrast on reflective surfaces, complicating accurate image interpretation. In contrast, back lighting is positioned behind the object relative to the camera, generating silhouettes that enhance contours and edges, making it ideal for precise dimension measurements and the inspection of cuts or perforations. The choice between these lighting methods should be made carefully, considering the object's specific characteristics and the requirements of the application, to optimize the visibility of critical details essential for effective analysis (HORNBERG, 2017).

2.3.1.2 Sensor

The process of image acquisition relies on hardware capable of capturing light and converting it into electrical charges. Central to this functionality are cameras, where the sensor plays a crucial role; it serves as the "eye"of the camera and is responsible for image generation. There are two main types of image sensors: Charge-Coupled Device (CCD) and Complementary Metal-Oxide-Semiconductor (CMOS). Each type of sensor has distinct advantages and is suitable for different applications, reflecting the diverse requirements of various imaging tasks in fields such

as computer vision, scientific research, and consumer electronics. Understanding the characteristics and performance of these sensors is essential for selecting the appropriate technology for specific imaging needs.

CCD sensors are semiconductor devices used for image capture in cameras and computer vision systems. Their operation is based on converting light into electrical signals through an array of photodiodes, where each pixel stores an electric charge proportional to the amount of incident light. After exposure to light, these charges are sequentially transferred to a central amplifier, where they are converted into digital signals. This serial transfer architecture allows CCD sensors to exhibit high signal uniformity and excellent image quality, with low noise levels and high sensitivity, particularly in low-light conditions. Consequently, CCD sensors are widely used in scientific and industrial applications that require precision in capturing details, such as in astronomy, microscopy, and high-resolution inspection systems (RUSS, 2007).

CMOS sensors are semiconductor devices characterized by the direct conversion of light into electrical signals at each pixel independently. Unlike CCD sensors, CMOS sensors have their own charge-to-voltage converter at each pixel, allowing the signal to be read in parallel, resulting in higher image capture speeds and lower power consumption. This integrated architecture also facilitates the inclusion of additional circuits, such as amplifiers and analog-to-digital converters, directly on the chip, reducing production costs. Although traditionally exhibiting more noise compared to CCD sensors, advancements in CMOS technology have significantly improved image quality, making them ideal for applications in smartphones, surveillance cameras, and industrial vision systems that require high speed and energy efficiency (RUSS, 2007).

2.3.2 Image Processing

An image can be defined as a two-dimensional function related to light intensity, $f(x, y)$, where x and y are spatial coordinates, and the value of f at (x, y) is proportional to the brightness at that point, which is referred to as a pixel in digital images. Manipulations applied to $f(x, y)$ are known as image processing, and refer to computational techniques applied to digital images to facilitate the extraction of meaningful information and support autonomous decision-making in subsequent stages. Image processing was developed to address three major challenges: image digitization and coding to facilitate transmission, printing, and storage; image enhancement to aid interpretation; and image segmentation, which is crucial in the early stages of machine vision (PETROU; PETROU, 2006).

2.3.2.1 Threshold

The thresholding technique is one of the most relevant approaches in image segmentation. In simplified terms, a threshold value is defined, and each pixel of the

image is evaluated to determine whether its value is above or below the established threshold. This process enables the creation of a binary image, reducing data complexity and facilitating object recognition and classification. However, segmenting images with more complex structures can pose a significant challenge in image processing, making this field of considerable interest and a constant focus of research. Generally, thresholding can be classified into three main types: global, local, and adaptive, each suited to different image conditions and characteristics (JYOTHI; K.BHARGAVI, 2014).

Global thresholding is used when objects of interest can be easily distinguished from the background, meaning the object and background values are consistent throughout the image. In this method, a single threshold value is applied uniformly to all pixels. Local thresholding, on the other hand, is employed when a single threshold value is insufficient for the entire image, which often occurs under non-uniform lighting conditions, such as in the presence of shadows. Shadows act as transition regions between the object and the background, making it difficult to find a single threshold value that works effectively in all shadowed areas. This technique divides the image into multiple regions, each using an appropriate threshold value for the pixels in that area. Finally, adaptive thresholding is used when a more sophisticated approach is required. In this method, a threshold value is calculated individually for each pixel, ensuring better results in situations where the distinction between object and background is not as clear (JYOTHI; K.BHARGAVI, 2014).

2.3.2.2 Noise

Image noise refers to the random variation of brightness or color intensity, representing an unwanted component that can compromise the quality and interpretation of the image. Noise introduces undesirable information into digital images, producing adverse effects such as unrealistic edges, lines, corners, and the presence of nonexistent objects, in addition to causing blurring and distortions in the background. Digital noise can originate from various sources, including Charge Coupled Device (CCD) and Complementary Metal Oxide Semiconductor (CMOS) sensors, which are commonly used in digital cameras (BOYAT; JOSHI, 2021).

The removal of noise from images is a critical component of image processing. An ideal noise elimination method should effectively eradicate noise while preserving the details of the original image. Noise removal techniques can be broadly classified into linear and nonlinear categories. Linear methods are characterized by their speed; however, they often fail to adequately preserve the finer details of the image. In contrast, nonlinear methods have the advantage of maintaining these details but tend to be more complex and may incur higher computational costs (VERMA; ALI, 2013). Consequently, it is essential to strike an appropriate balance between the desired level of precision, computational expense, and the time required for program execution,

ensuring that the chosen approach aligns with the specific application requirements.

2.3.2.3 Filters

Filters are widely used to improve image quality, facilitating more accurate and effective analyses. Considering an image as a matrix of values that represent the brightness of each part of the image, any algorithm that manipulates pixel values can be classified as a filter. In general, pixel values are modified based on the values of neighboring regions, resulting in enhanced image quality and the highlighting of certain features, thereby aiding future analyses.

Obtaining a high-quality image is essential for conducting effective analyses, and in this context, filters play a crucial role. In addition to enhancing the most important parts of the image for subsequent analysis, filters are also employed for noise reduction. The algorithms responsible for noise removal typically operate by smoothing the entire image while preserving areas near contrast boundaries, which reduces the visibility of noise. However, these same algorithms may also decrease the visibility of details that, although not highly pronounced, are still significant for future image analyses (VERMA; ALI, 2013). Therefore, it is vital to carefully assess the noise present in images to choose the most appropriate filter that allows for its removal without compromising the preservation of important details.

2.3.3 Image Analysis

Image analysis refers to the process of extracting meaningful information from digital images or videos through the application of computational techniques. This process involves interpreting the content of the image by recognizing objects, patterns, or other characteristics, thereby enabling automated decision-making based on the objectives of the project.

2.3.3.1 Template Matching

In most applications of object detection in computer vision problems, it is necessary to define similarity parameters between the objects or patterns present in the images under analysis. One of the most commonly used techniques for this purpose is template matching. This image analysis technique aims to determine whether a specific object of interest appears in the image and to identify its location. To achieve this, a template of the object of interest is utilized, which is then slid across the entire image to check for the presence of the object. The position that provides the best match between the template and the analyzed portion of the image is returned as the location where the object is found. If there are no regions in the image that correspond well to

the template, it is concluded that the object is not present in the image (HASHEMI et al., 2020).

2.3.3.2 Circles

Pattern recognition is essential for image analysis, particularly in optical systems, where components typically have circular shapes. Although template matching is an efficient technique for identifying various types of objects, more direct methods can be applied for detecting simple geometric shapes, such as circles. In this context, the Hough Transform is an effective approach for circle detection (KUO et al., 2019), offering stable performance and ensuring the repeatability of the process, a critical feature for accurate analysis in optical systems.

3 METHODOLOGY

This section describes the materials and methods used in the automated construction of a lens system for use in endoscopes. The system aims to automate the production of lenses for small cameras employed in endoscopy, utilizing an approach that incorporates plastic lenses, which helps reduce costs. The system's accessibility allows for the replacement of endoscope tips between uses with different patients, a crucial factor in preventing infections and diseases related to the use of these devices. Although current cleaning methods are effective, they are not entirely reliable. However, the use of plastic lenses presents challenges due to their small size and inferior optical properties compared to glass lenses. Therefore, the assembly process must be highly precise to compensate for the material's lower performance and ensure the system operates efficiently.

Figure 12 – Autocollimator and Micromatipulator Stand (AMS).

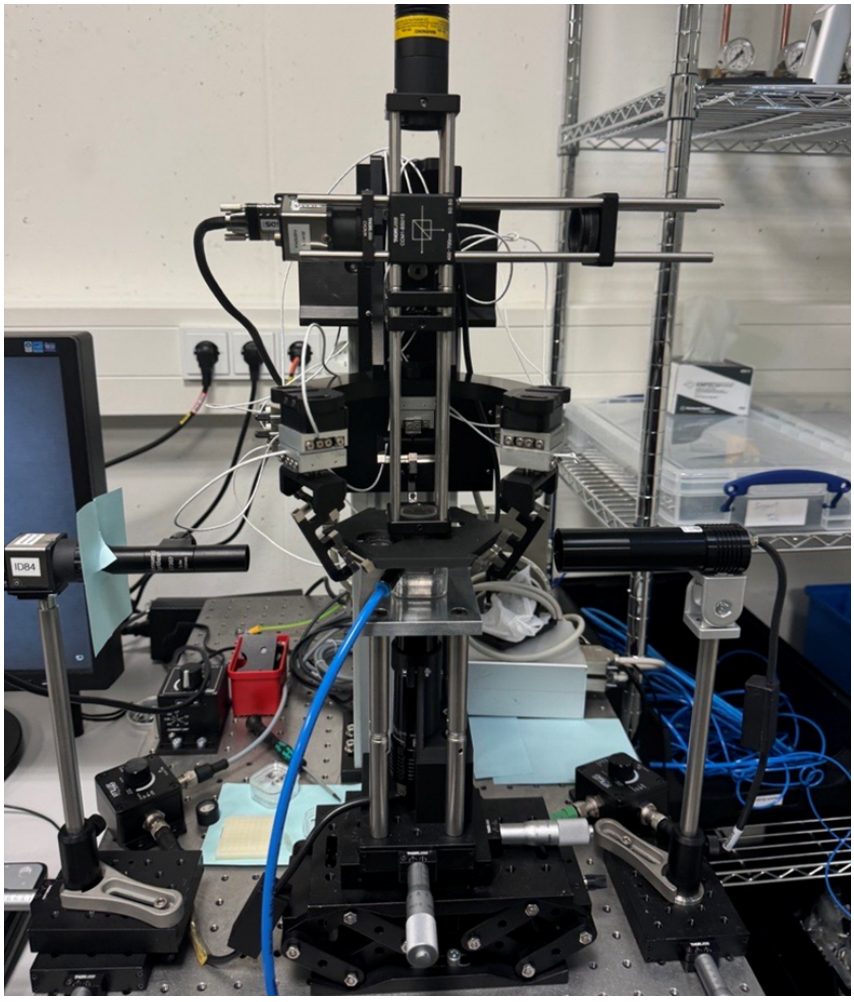

Source: Author (2024).

The configuration of the automated system for the production of lenses used in endoscopes consists of two main modules. The first module, called the Autocollimator and Micromanipulator Stand (AMS), illustrated in Figure 12, is dedicated exclusively to the precise positioning of the lenses, ensuring absolute flatness and the absence of tilt or deviation. Additionally, it guarantees that each lens is correctly positioned along the reference axis, which is essential for the optimized alignment of all optical components. The second module, known as the Lens Assembly Station (LAS), is responsible for securing the lenses and the iris using an adhesive. In this process, the initial module positions the lens in the appropriate location and then transfers it to the subsequent module, where it is securely fixed through the application of an adhesive substance. This procedure ensures the stability and permanence of the alignment, safeguarding the integrity and continued functionality of the optical system after assembly.

Within the scope of this work, only the AMS module will be addressed, with a focus on manipulating the lenses to ensure they are aligned in the correct position. The complete optical system consists of multiple lenses and an iris; however, this study will present the methodology for assembling just one lens with the iris. For the full construction of the system, this process must be repeated for each additional lens, progressively mounting the lenses onto the previously assembled structure. This procedure requires an auxiliary structure to hold the components in place and facilitate layered assembly, forming a "lens tower"that constitutes the complete optical system.

The characteristics of the lens to be manufactured and the structure used in the process will be detailed.

3.1 LENS SYSTEM

Figure 13 – Lens System.

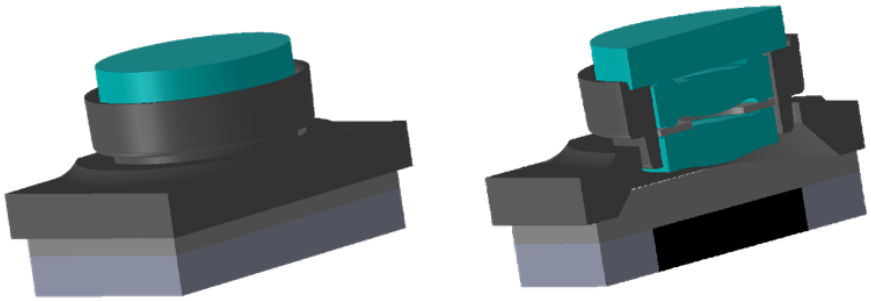

Source: Adapted by the author (2024).

The proposed optical system consists of four parts: three lenses and an iris. The entire system is encapsulated in an external structure that ensures the lenses

remain fixed in the correct positions after assembled. This structure, along with its lateral cut, allows for a better visualization of the lenses and the iris, as illustrated in Figure 13. As explained at the beginning of this section, the focus of the methodology is on the iris and the lenses that are fixed to it.

Figure 14 – Lens Datasheet.

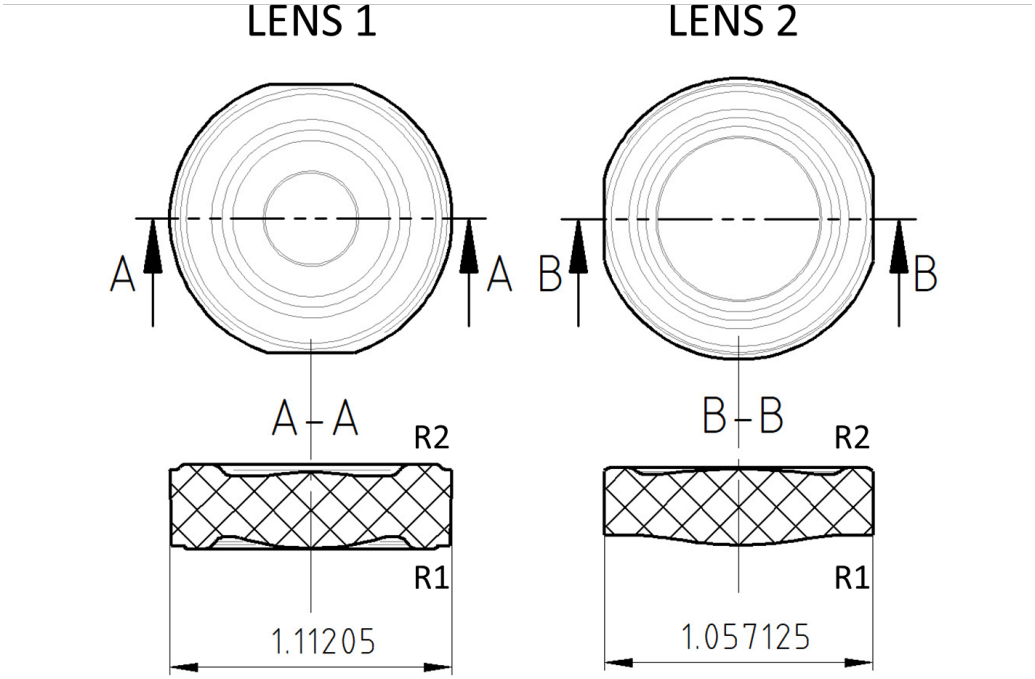

Source: Adapted by the author (2024).

The iris is a small circular structure with a diameter of 1.1 millimeters and features a central circular opening of 0.5 millimeters. Both lenses, which are biconvex, have a diameter similar to that of the iris, as illustrated in Figure 14. The respective radius of the lenses is presented in Table 1, and it is important to note that Lens 2 is aspheric; thus, its radius 1 is not constant, with only the base radius represented in the table.

Table 1 – Lens Radius.

Lens	Radius 1 (mm)	Radius 2 (mm)
Lens 1	1.000	1.130
Lens 2	1.100	2.500

Source: Author (2024).

3.1.1 Lens Integrity

The lenses in question are embedded in plastic molds, as illustrated in Figure 15, and must be extracted from these molds before being used in the construction of

the optical system. An important concern during this process is the risk of damaging the lenses during removal, as their small size makes them particularly sensitive to damage. Therefore, careful handling is necessary to ensure that the integrity of the lenses is preserved throughout this process.

Figure 15 – Lens Mold.

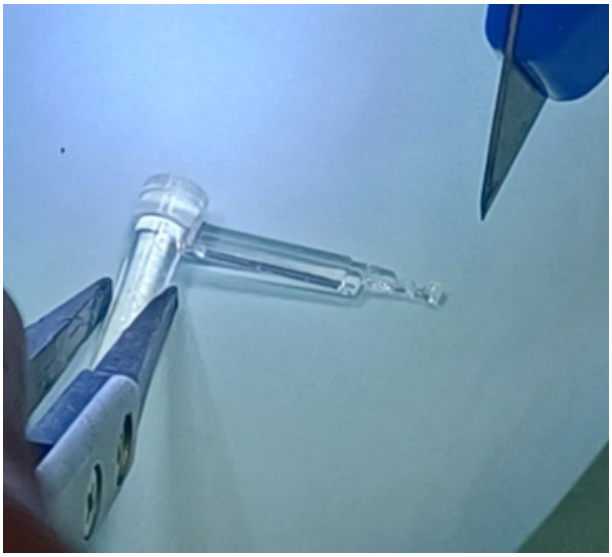

Source: Author (2024).

Figure 16 – Lens Internal Pressure Measurement.

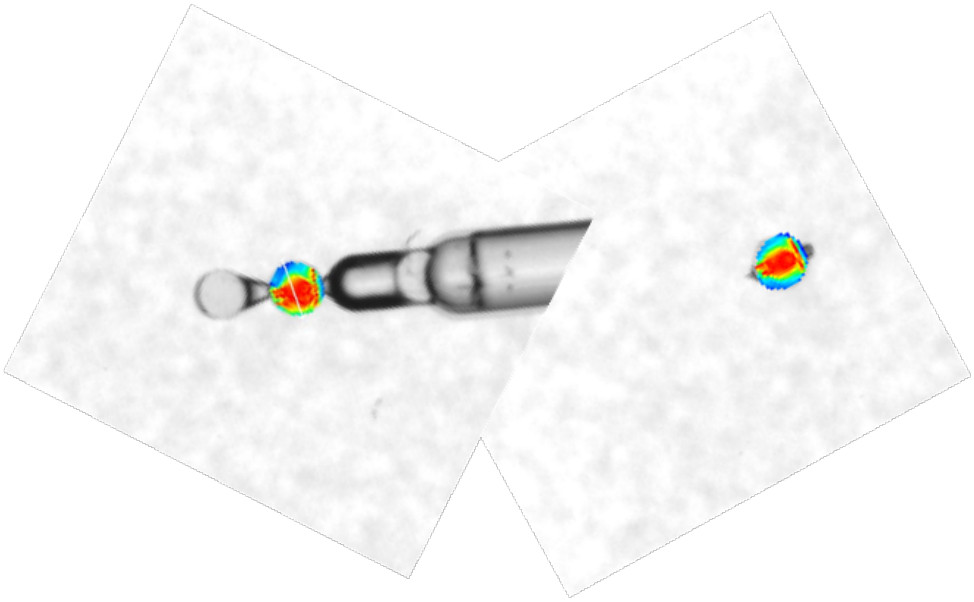

Source: Author (2024).

The proper functioning of the optical system relies on the integrity of the lenses, particularly to compensate for the inferior optical properties of plastic. Therefore, it is crucial that the lenses are extracted from their molds without sustaining damage.

One way to verify the integrity of the lens after extraction is by measuring the internal pressures. In this study, an analysis of the internal pressures was conducted before and after the removal of the lenses from the mold. The results, presented in Figure 16, indicate that there were no significant changes in the internal pressures, suggesting that the lens remained intact and ready for use.

3.2 STRUCTURE

Figure 17 – Autocollimator and Micromanipulator Stand (AMS).

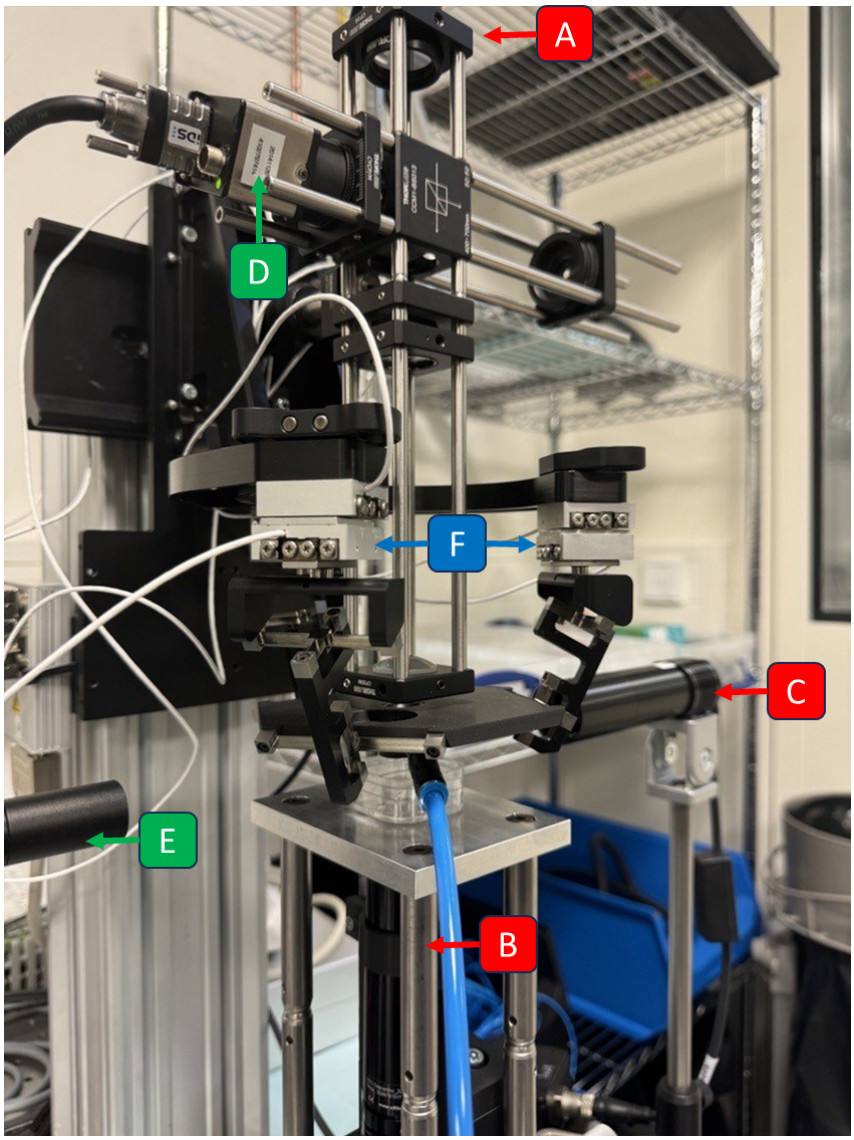

Source: Author (2024).

To manipulate the lenses and the iris, a highly precise actuator and an appropriate measurement system are required due to the small size of these structures, as explained in Section 2.2. For this purpose, the Autocollimator and Micromanipulator Stand (AMS) is utilized, which is equipped with an autocollimator, two cameras, and

three distinct light sources. The structure of the AMS and its divisions are presented in Figure 17; parts A, B, and C correspond to the light sources of the system, parts D and E correspond to the cameras, and part F corresponds to the actuator, the Commander 6.

3.2.1 Autocollimator

As previously outlined, the autocollimator is of paramount importance in acquiring data for the lens alignment process. The system consists of a camera and an optical apparatus designed to collimate the incoming light and subsequently focus it on the lens of interest. This methodology enables the calculation of the lens positioning through a technique analogous to that described in Section 2.2.

Figure 18 – Autocollimator Schematic.

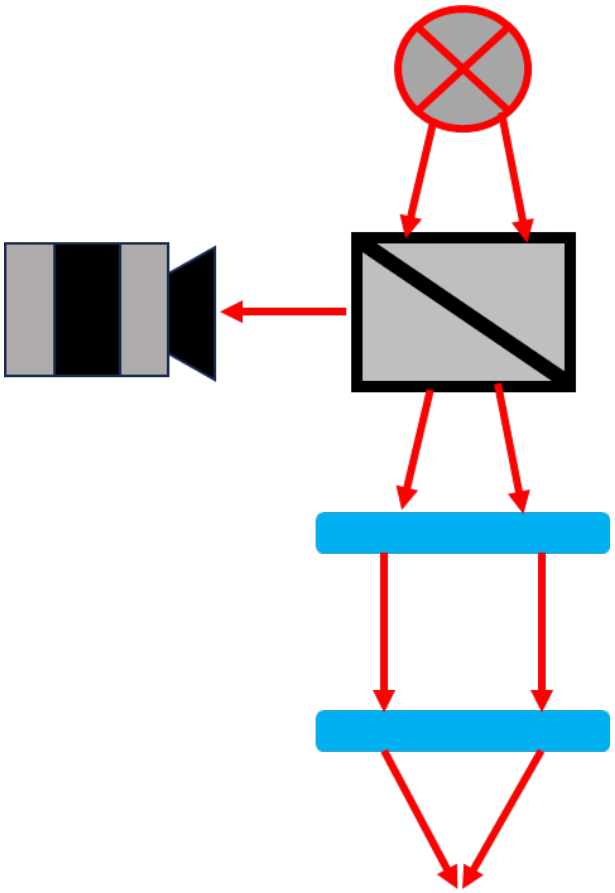

Source: Author (2024).

The autocollimator in question utilizes an X-shaped LED illumination that passes through a beamsplitter, allowing the light to reach the object of interest (the lens) while also being reflected to a camera, enabling data recording. After passing through the beamsplitter, the light travels through a collimating lens with a focal length of 150 mm, which ensures the rays are parallel. Following this, the light passes through a lens

with a focal length of 30 mm, responsible for focusing the light on the lens of interest. A schematic of the autocollimator's operation can be seen in Figure 18.

3.2.2 Cameras

The system consists of two cameras. The first, referred to as the autocollimator camera (D in Figure 17), is directly attached to the autocollimator and is responsible for detecting parameters such as the lens positioning, flatness, tip, and tilt. The second camera, called the "side camera"(E in Figure 17), is positioned laterally to monitor the alignment of the lens with other optical components, such as another lens or an iris. Table 2 presents technical specifications for the cameras used in this setup. Both cameras are of the same model, so the information provided applies to each camera.

Table 2 – Camera datasheet information.

Manufacturer	IDS
Sensor type	CMOS Mono
Resolution (h x v)	1280 x 1024 Pixel
Pixel size	5.3 µm

Source: Author (2024).

3.2.3 Ilumination

To facilitate enhanced visibility during the lens preparation process, the module incorporates three distinct telecentric sources of illumination. The first source, attached to the autocollimator (A in Figure 17), emits a cross-shaped beam of light that traverses the optical system, concentrating its illumination on the lens being manipulated. The second source of illumination (C in Figure 17) is directed towards the lateral aspect of the lens, enabling the side camera to capture images with sufficient clarity for alignment checks. The third source (B in Figure 17) provides illumination from below, facilitating the measurement of the positioning of the base component where the lens will be mounted.

3.2.4 Gripper

An essential part of the design consists of grippers capable of holding the components of the optical system that will be manipulated. Two grippers are used: one to hold the lenses, which is attached to the Commander 6 actuator, and another to hold the iris, located below the actuator. Both grippers are designed to securely grasp the small structures of the lenses and iris while allowing light to pass through them, enabling image capture by the autocollimator camera.

Figure 19 – Light Passing Through the Grippers.

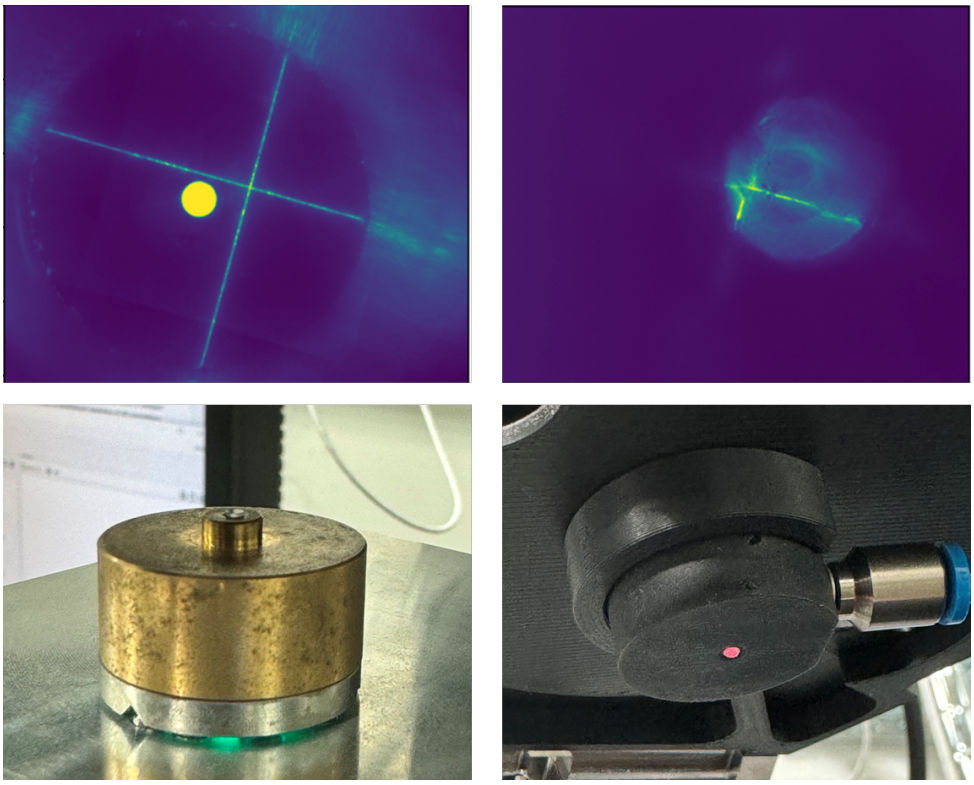

Source: Author (2024).

The lens gripper enables the transmission of light from the autocollimator (labeled as A in Figure 17), allowing it to be detected by the autocollimator camera. Similarly, the iris gripper allows passage of the lower light (labeled as B in Figure 17) to be captured by the autocollimator camera. An image captured by the autocollimator camera through this configuration is shown in Figure 19. In the top-right section of the image, light from the autocollimator can be seen reflected off the lens surface. The top-left section displays the light passing through the central aperture of the iris as well as the light reflected from the iris surface. In the lower portion of the image, a photo of the iris gripper is shown on the left, while a photo of the lens gripper appears on the right.

3.2.5 Commander 6

The micromanipulator Commander 6 (C6), developed by Fraunhofer IPT, is designed to align optical elements across six degrees of freedom, thereby enhancing precision in lens assembly. The C6 employs three piezo linear actuators with titanium solid-state hinges, enabling exceptional positional accuracy within a compact framework. This configuration achieves a translational resolution of 50 nanometers, along with a rotational resolution of 1 microradian, while maintaining a translational repeatability of 150 nanometers. It is also possible to redefine the origin of the actuator's

coordinate system to facilitate the positioning of manipulated objects.

In the process analyzed in this work, the Commander 6 is used to position the lens so that it is entirely flat and centered in relation to the iris, as illustrated in Figure 20. As can also be seen in the image, the origin of the coordinate system has been adjusted to be at the lens of interest being moved by the actuator.

Figure 20 – Commander 6 Coordinate System.

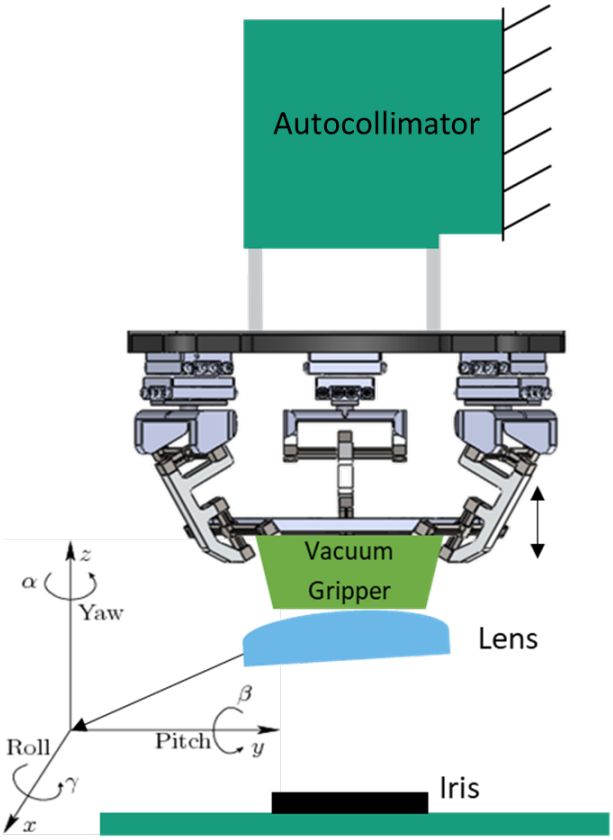

Source: Author (2024).

4 DATA PRESENTATION AND ANALYSIS

This section presents the data collected throughout the project, along with a detailed description of each step of the processes employed and an analysis of the results achieved. The primary objective of this study is to automate the lens construction process for endoscopes and evaluate the precision achieved by this automation. The system implementation requires a series of well-organized steps to ensure both efficiency and accuracy in the final outcome.

The assembly of the optical system requires defining a reference base axis, where both the iris and the lens will be centered, ensuring the correct assembly of the system. The first step involves positioning the iris in its gripper and measuring its center to serve as the base axis. Next, the lens is placed in its gripper, and its centers of curvature are identified and used to calculate the lens center, following a measurement technique similar to that described in Section 2.2.

After the initial calculations, the lens is adjusted so that its center precisely coincides with the reference axis, ensuring that it is centered relative to the iris. In the final step, the iris and the lens are moved closer until they are nearly in contact, and the central alignment of both components is verified using a lateral camera within the system. This procedure ensures proper alignment between the parts, which is essential for the accuracy of the assembled optical system.

4.1 IRIS IDENTIFICATION

The first step in the process is the identification of the iris. For this, the iris is positioned in its gripper, and the lower light (B in Figure 17) is activated, allowing the light to pass through the inner aperture of the iris and be visualized by the autocollimator camera. Since this camera is used to capture the image, the internal optical system of the autocollimator, as described in Section 3.2.1, causes the image to focus only at a specific distance of 30 mm from the lower lens. Thus, the position of the iris must be adjusted to reach this focal distance, ensuring a sharp visualization.

To confirm that the iris is correctly positioned at the focal point, the cross-shaped light of the autocollimator (A in Figure 17) is used. When the “X” projected by the light appears sharply, it indicates that the iris is properly aligned. With the iris correctly focused, the Hough Transform, as described in Section 2.3.3.2, is applied to identify the contour of the iris circle. This procedure allows for the precise location of the iris center, which will serve as a reference position for aligning the lens.

The illustration provided in Figure 21 presents three stages of the process: on the left, the image shows the light passing through the iris while it is still out of

optimal focus; in the center, the light when the iris is in the correct position, with the autocollimator “X” sharply focused, indicating that the focal point has been achieved; and on the right, the circle identified by the Hough Transform, along with the marking of the center. This center will be used as the reference point for precise alignment and union between the lens and the iris in the next stage of the assembly process.

Figure 21 – Iris Identification.

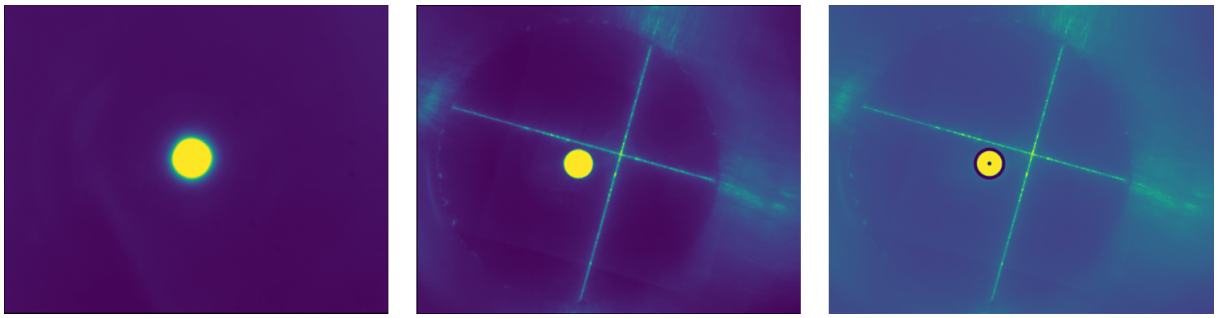

Source: Author (2024).

4.2 LENS IDENTIFICATION

After identifying the iris and ensuring its proper positioning, the next step in the process is the identification of the lens. To carry out this stage, the lens is positioned in its gripper, and the Commander 6 actuator is used to manipulate it in the x/y plane defined in Figure 20, facilitating visualization by the autocollimator camera. Additionally, the actuator is also employed to move the lens in the z direction, improving its visibility by aligning it to the focus of the autocollimator’s optical system. This adjustment is essential to ensure that the resulting image is sharp and clear.

Figure 22 – Lens view by autocollimator and side camera.

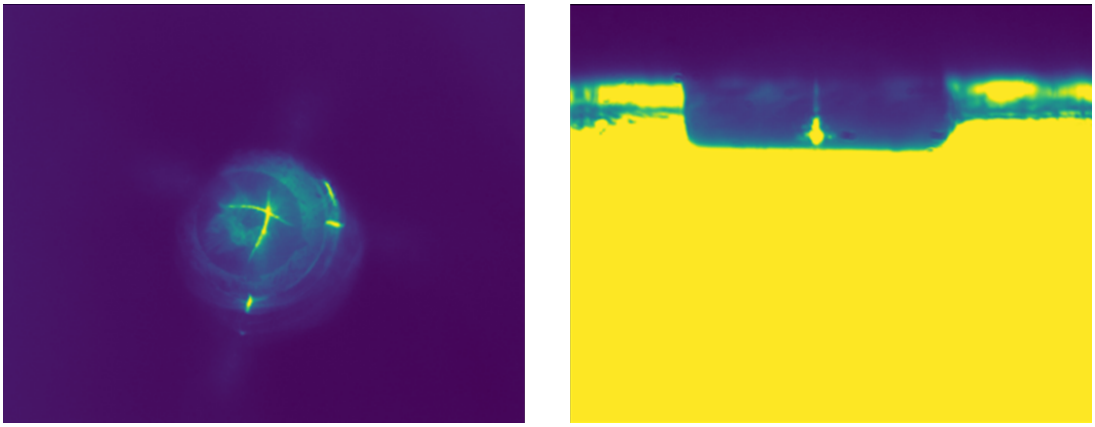

Source: Author (2024).

An image of the lens captured by the autocollimator camera is presented in Figure 22. The concentration of light, as illustrated in the left side of Figure 18, occurs near the lens' surface, which is a critical factor for the quality of the resulting image. Proper lighting is essential for ensuring accurate positioning of the lens. Additionally, the right side of the figure features an image from the side camera, providing an alternative perspective that enhances the understanding of the lens's structure and its placement within the optical system.

With the lens positioned within the camera's field of view (FOV), scanning along the z-axis becomes necessary to locate the centers of curvature. This is accomplished using a measurement technique similar to that described in Section 2.2. When the autocollimator light is focused on either the lens surface or one of its curvature centers, a cross generated by the illumination becomes visible. This visual cue confirms that the measurement point is accurate, ensuring reliable data collection for subsequent analysis. Figure 23 illustrates the trajectory taken during the scanning process along the z-axis. The lens depicted in the image is lens 1, with its radii detailed in Table 1. The points marked with an "x"correspond to the positions where the crosses generated by the autocollimator light are expected to be visible. These points represent the curvature center of radius 1, the lens surface, and the curvature center of radius 2, respectively.

Figure 23 – Lens scan on z axis.

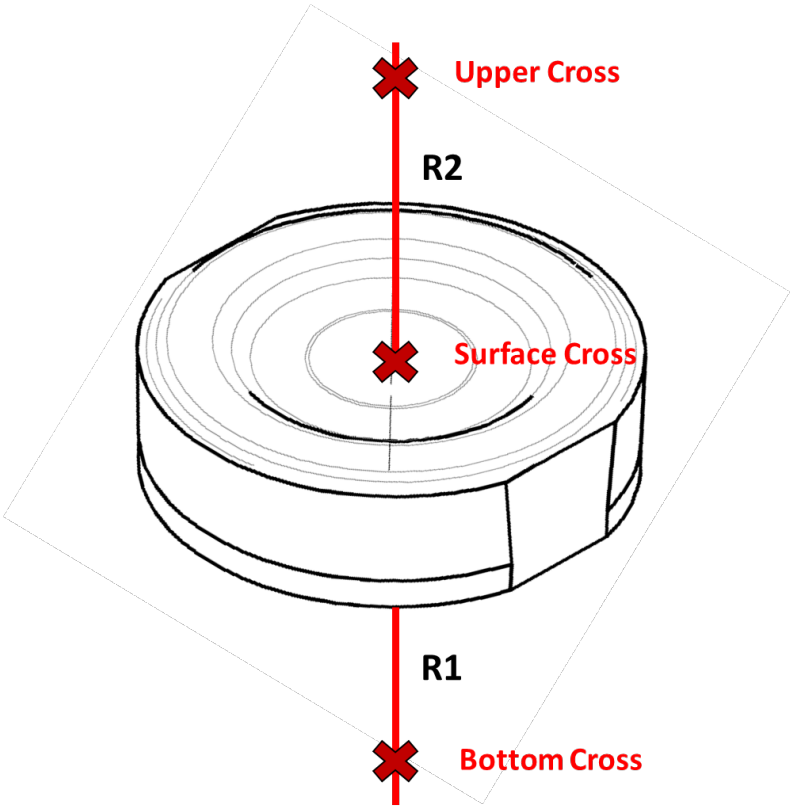

Source: Author (2024).

An image of the data obtained from this scanning process is presented in Figure 24. On the y-axis, the variable "signal"is represented, indicating the intensity of the match between the image captured by the autocollimator and a cross template used in a template matching function. Therefore, the higher the signal value, the more similar the collected image is to the provided template. This metric is crucial for assessing the accuracy of the lens alignment, as it directly reflects the effectiveness of the scanning process and the quality of the acquired images.

On the x-axis, the steps of the scanning along the z-axis are represented, with intervals of 0.1 mm, totaling a range of 2.5 mm. In this specific case, lens 1 was scanned, and this range of 2.5 mm is sufficient to ensure that both the curvature centers of the lens and its surface have been adequately covered during the process. The selection of this range is fundamental, as it ensures that all relevant regions of the lens are analyzed, allowing for a comprehensive evaluation of its optical characteristics. Furthermore, the lines presented in the graph indicate the points considered by the algorithm as the locations where the generated crosses were identified, corresponding to the curvature centers of the lens rays and the surface.

Figure 24 – Scan on z axis.

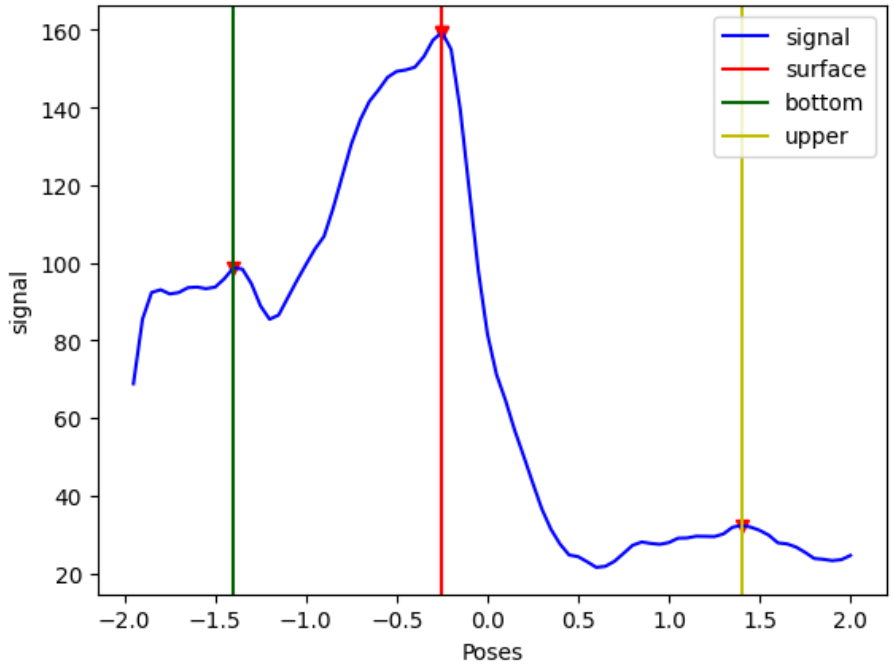

Source: Author (2024).

To determine the positioning of the curvature centers of the rays and the surface of a biconvex lens, it is essential to analyze data obtained through the template matching technique, which employs a cross-shaped template on images captured by the autocollimator camera. When light passing through the optical system of the autocollimator is focused on the lens surface, the resulting image is more intense due

to direct reflection, with the highest peak on the graph corresponding to this surface position.

In contrast, the formation of the cross at the curvature centers of the lens rays has distinct characteristics. In this case, only a fraction of the light is reflected back, and this occurs when the light strikes the lens at an almost perpendicular angle, as explained in Section 2.2. This results in a less intense image and a weaker signal when processed by the template matching function. Regarding the curvature center of the ray located below the lens (R1 in Figure 23), the light must pass through the lens to reach this center, and any tilt or imperfections on the surface cause light refraction, increasing noise in detection, as illustrated in Figure 24.

Once the signal graph is obtained and considering the behavior of light and associated noise, data processing is necessary to achieve more accurate results. The first step involves smoothing the graph, which helps minimize errors caused by small lighting variations and makes it easier to identify more reliable signal peaks. Following this smoothing process, the main peak—corresponding to the surface—is identified, as it represents the highest intensity point on the graph. It is important to note that since the lens surface is not perfectly flat, the point located may not exactly match the real surface.

With the surface position identified and data from the lens presented in Table 1, it is possible to estimate where the other curvature centers should be located, as these points are specified. The analysis thus prioritizes regions on the graph where the cross formations are expected, allowing a tolerance to account for potential inaccuracies in surface positioning and variations in the specified curvature centers. This tolerance is necessary, as the lens, being small and made of plastic, may present non-ideal optical properties. Furthermore, for precise results, the lens would need to be perfectly flat, which is not always feasible.

Figure 25 – Detected crosses.

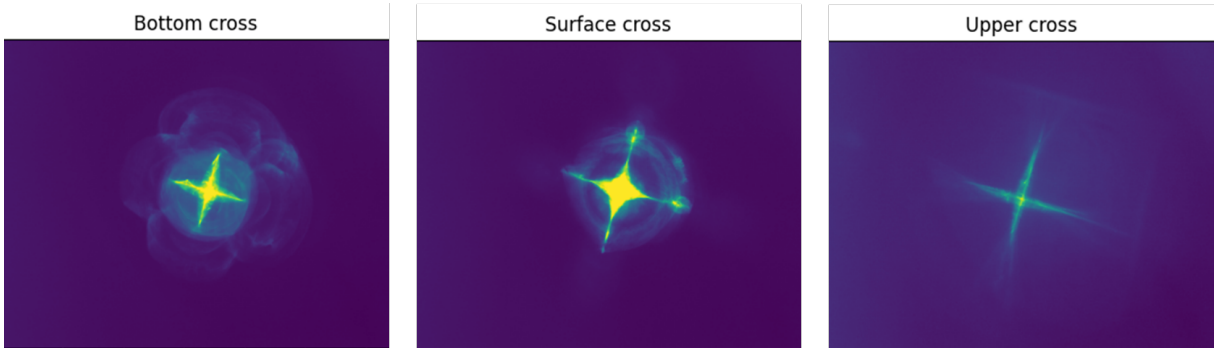

Source: Author (2024).

Once the crosses are located, template matching is applied again to find the centers of the generated crosses. These central points can then serve as a reference

to determine the lens positioning. Unlike the technique explored in Section 2.2, no rotation of the lens is performed. Instead, with the central point of the cross identified at each curvature center, a line can be drawn between the two points, and the midpoint of the lens can be calculated, identifying the point that represents the center of the lens.

It is important to note that if the calculated centers of the crosses do not align on the same pixel in the image obtained by the autocollimator camera, the lens will not be perfectly flat, introducing errors in aligning the lens with the iris. Further details on this issue, as well as potential solutions and their outcomes, will be discussed in Section 5.

4.3 ALIGNING THE IRIS AND LENS

Once the lens and iris are identified, it is necessary to align the two structures so that they are both centered. As previously mentioned, the position of the iris serves as the reference for this alignment. The pixel representing the center of the iris aperture through which light passes, illustrated in Figure 21, is stored and used as the reference point. With the iris position defined, it is necessary to move the lens until the midpoint, determined by the intersection of the crosses formed at the curvature center regions, aligns with the same pixel as the iris. In other words, the center of the lens must coincide with the center of the iris.

Figure 26 – Side View of Lens and Iris.

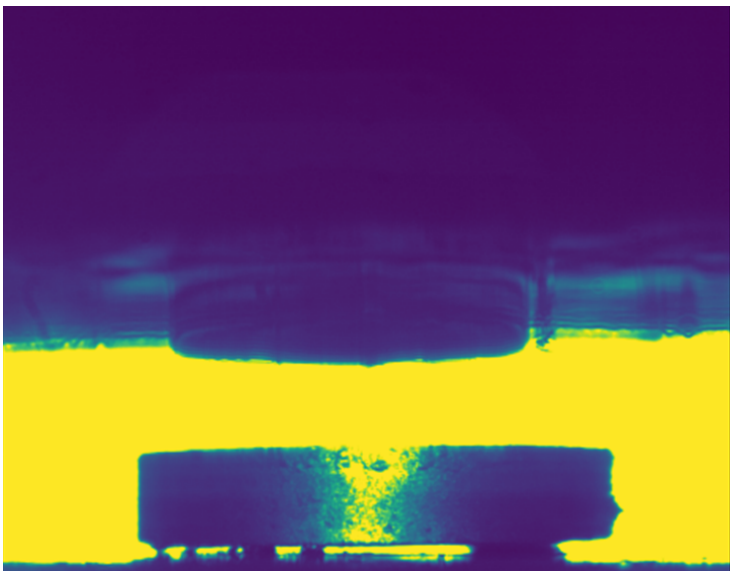

Source: Author (2024).

In Figure 26, the iris and lens can be seen after being aligned according to the process described. The lens movement is controlled by the Commander 6 actuator, which has sufficient precision to position the lens correctly. However, it is necessary to

adjust the actuator's coordinates to move the lens within the same coordinate system displayed in the image captured by the autocollimator camera. Additionally, the magnification caused by the lenses used in the optical system of the autocollimator must also be taken into account. With these considerations in place, the precise alignment of the lens and iris can be achieved.

4.3.1 Adjustment of the Commander 6 Coordinates

The coordinate system of the Commander 6 actuator does not align with the coordinate system of the image captured by the autocollimator camera. When the actuator is moved along the x or y axes, the movement observed in the camera appears diagonal, which complicates the precise alignment of the lens with the iris. To simplify this alignment process, it is advantageous to adjust the x and y directions so that they match between the camera and actuator coordinates. This way, when it is determined that the lens needs to be moved a specific distance along the x-axis, no additional calculations will be required to decompose this movement into the x and y coordinates of the autocollimator system, making the lens positioning process more straightforward and efficient.

Figure 27 – Camera x C6 coordinates.

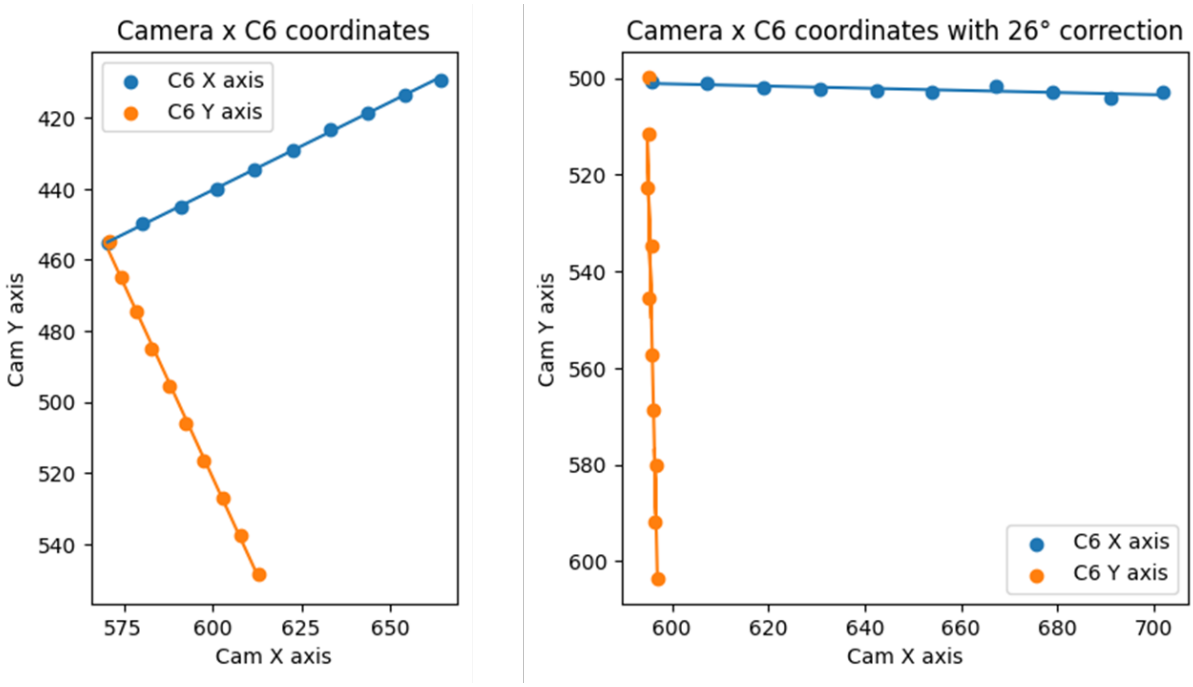

Source: Author (2024).

To perform the adjustment, the actuator moved the lens until it was focused on the cross formed above the lens. Then, the actuator was displaced along the x-coordinate in constant step sizes, with an image being captured at each movement.

This process was repeated by moving the actuator along the y-coordinate. After capturing the images, the template matching technique was applied to locate the center of the cross, and the results were plotted in the graph on the left side of Figure 27. As can be observed, the coordinate system of the Commander 6 actuator exhibits a slight rotation relative to the coordinate system of the camera.

Based on the obtained results, two lines were drawn to best fit the identified points, and the angle of inclination of these lines was calculated. This value was then used to adjust the actuator's configuration, aiming to more precisely align the two coordinate systems. The adjustment was made with an inclination of approximately 26 degrees along the x-axis, with the result shown on the right side of Figure 27. Although the coordinate systems are now well aligned, the alignment is still not perfect. The inclination calculation was repeated, revealing a residual difference of around 1 degree. However, the previous adjustment was maintained, as small variations in the calculations can occur due to factors such as lighting fluctuations and noise, which affect the accuracy of the cross-center identification and make it difficult to achieve perfect alignment.

4.3.2 Autocollimator's Magnification

Before performing the actuator movement, it is essential to consider the magnification produced by the optical system of the autocollimator, which results from the lenses used in this device. Ignoring this magnification could lead to incorrect interpretations of the displacement, as actuator movement may produce a perceptibly larger shift in the captured image. To precisely calculate the magnification of the autocollimator's optical system, it is critical to have detailed data on the lenses used. Table 3 presents the main characteristics of these lenses.

Table 3 – Autocollimator Lens data.

Lens	Focal Lenght (mm)	Tolerance (%)
Lens 1	150	1
Lens 2	30	1

Source: Author (2024).

With this information, it is possible to calculate the system's magnification. In this specific setup, the object (light in the shape of an X) is positioned at the focal distance of the first lens, which projects its image to infinity, collimating the light rays, that is, making them parallel. The second lens then focuses this light at its focal distance, as illustrated in Figure 18. In this configuration, magnification can be determined by Equation 3, where M represents magnification, F_1 denotes the focal length of lens

1, and F_2 is the focal length of lens 2. Using the information provided in Table 3, a magnification of 5x is obtained.

$$M = \frac{F_1}{F_2} \tag{3}$$

4.3.3 Move the lens to match the iris position

After adjusting the coordinates of the Commander 6 actuator relative to the camera's coordinate system and calculating the optical magnification of the system, it is possible to precisely position the lens to align it with the iris. First, the distance in pixels between the point considered the center of the lens and the center of the iris is calculated. This difference is then converted into millimeters by multiplying the pixel count by the camera's pixel size, based on the technical data presented in Table 2. The resulting millimeter distance is divided by the autocollimator's magnification, providing the real distance between the two reference points. This information is then used by the Commander 6 actuator to correct the lens position.

Figure 28 – Iris and lens prior to alignment.

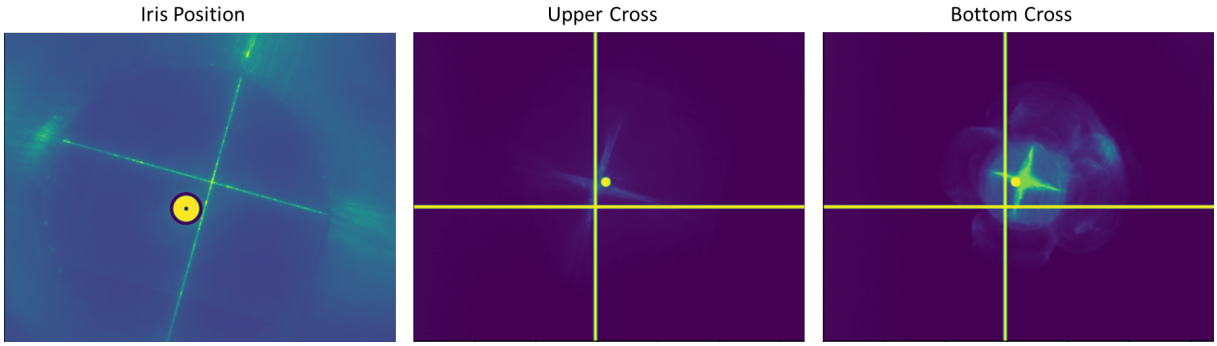

Source: Author (2024).

Figure 28 shows the iris positioning on the left, used as a reference for alignment with the lens. The middle and right images display the upper and bottom crosses, respectively, with a yellow point indicating the calculated center of the lens, and two lines forming a cross representing the central position of the iris, which is the target position for the lens. After the adjustment performed by the Commander 6 actuator, Figure 29 shows, on the left and the middle, the final alignment of the upper and bottom crosses, with the yellow point on the lens aligned with the iris position. The image on the right, captured by the side camera, shows the alignment of the lens and iris following the process.

Figure 29 – Iris and lens after alignment.

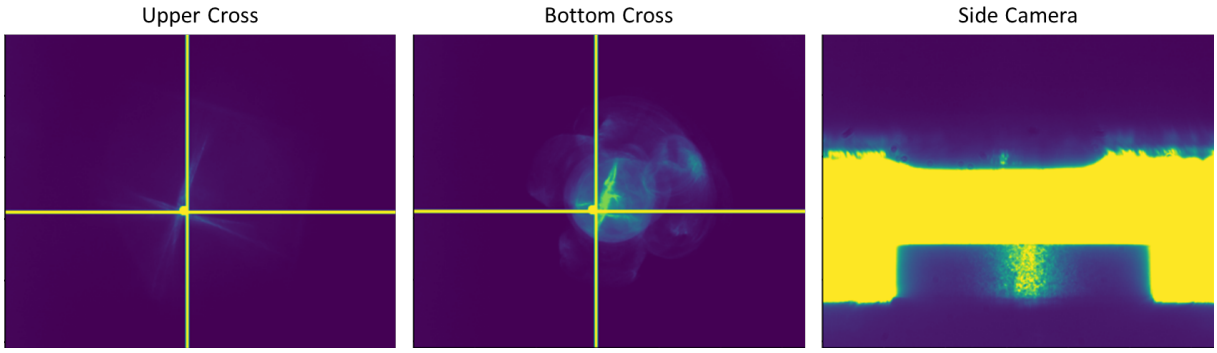

Source: Author (2024).

4.4 PROCESS EFFICIENCY ANALYSIS

To evaluate the efficiency of the process, the procedure was repeated five times. In each iteration, the lens and iris were removed and reinserted into the gripper, simulating the replacement of new parts. The efficiency analysis is based on the lens's centralization, observed through the image obtained from the side camera (side cam), as shown in Figure 26. This image provides a view of one side of the lens and serves as a partial alignment reference. However, it is important to note that the side camera does not provide depth alignment information. This limitation implies that the lens may appear centered in the side view but still exhibit misalignment along the depth axis. Despite this, the side view remains a practical and useful metric for evaluating process efficiency, aiding in the identification of inconsistencies and potential systematic deviations. The results obtained from this methodology are presented in the graph in Figure 30, providing an analysis of the process efficiency.

Figure 30 – Placement error between lens and iris.

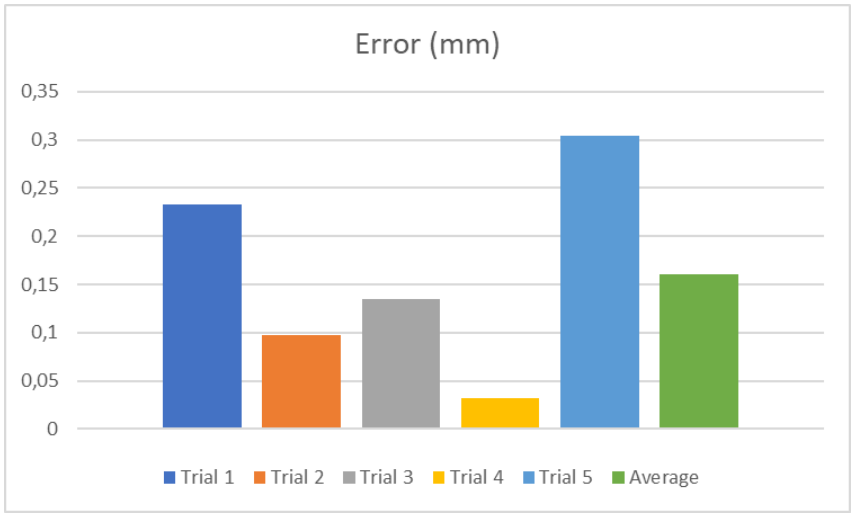

Source: Author (2024).

The errors observed in the tests likely stem from certain process inaccuracies, such as the misalignment between the camera's coordinate system and that of the Commander 6 actuator. Additionally, minor lighting variations may influence the calculation of the lens center, subtly shifting the position determined by the template matching of the crosses.

Another important factor to consider is the initial positioning of the iris within the system. If the iris is too far from the point where the autocollimator's illumination projects the X pattern, correctly positioning the lens becomes challenging. This occurs because, when the lens is moved away from this ideal point, identifying the crosses formed on its surface becomes more difficult, as illustrated in Figure 29, where the lower cross is barely detected. This phenomenon is due to the specificity of the cross formation point, as it is essential for the autocollimator's light to be focused by the optical system in a very precise area; otherwise, the crosses are not visible. Therefore, positioning the iris as close as possible to the area where the autocollimator focuses its illumination is crucial, as it facilitates lens manipulation and allows for accurate cross localization.

Figure 31 – Side camera image of trial 3.

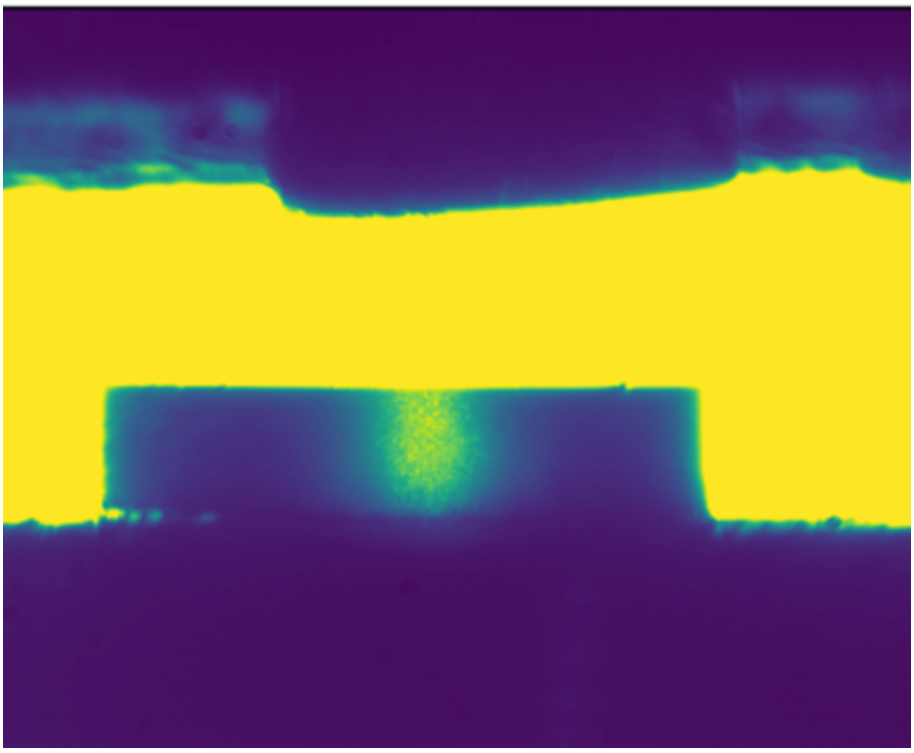

Source: Author (2024).

The primary source of error, however, is the tilt of the lens. Close observation of Figure 28 reveals that the yellow dot, indicating the calculated center of the lens, is not precisely centered relative to the upper and lower crosses, suggesting a slight lens tilt. If the lens were completely flat, the crosses would form in the exact same position.

This issue will be explored in greater detail in Section 5, where an additional procedure is presented to ensure proper flat positioning of the lens. In the trials that exhibited the highest errors, the lens was noticeably tilted, similarly as illustrated in Figure 31.

5 IMPROVEMENTS

The efficiency of the process, presented in Section 4.4, shows significant potential for improvement. The factors responsible for the reduction in accuracy, previously discussed, will be addressed in this section with proposed solutions for their mitigation. Furthermore, at the end of this analysis, new efficiency tests will be conducted using the same methodology applied earlier to verify whether the implemented changes have effectively improved the process performance.

5.1 LENS TILT CALCULATION

Figure 32 – Lens tip and tilt vector.

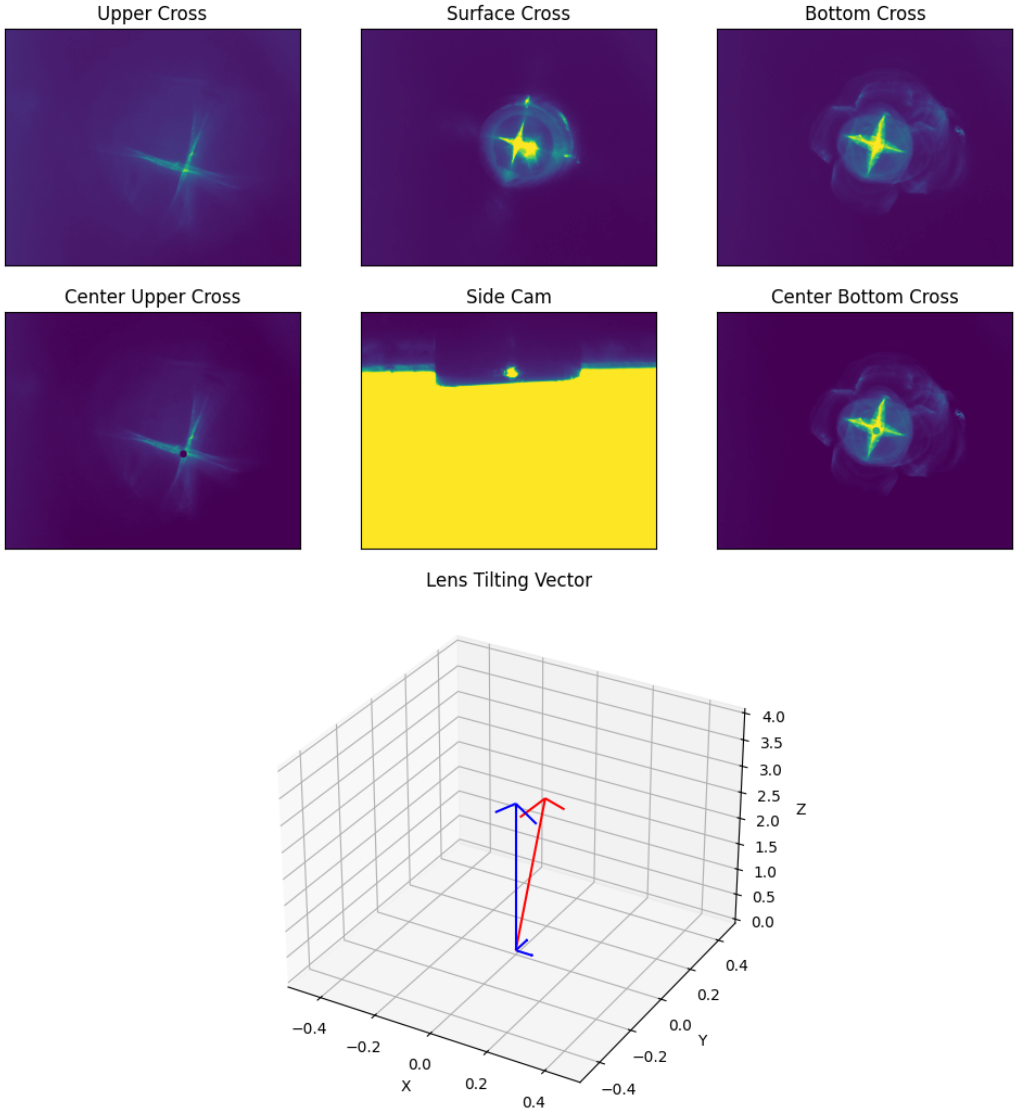

Source: Author (2024).

The calculation of the lens tilt was performed similarly to the procedure used to determine the lens center during the alignment process between the lens and the iris, described in Section 4.2. This process began with a scan along the z-axis to identify the crosses formed at the centers of curvature of the biconvex lens. After locating these crosses, their centers were determined using template matching techniques. The resulting data, combined with the coordinate information obtained during the scan, provided the necessary parameters to calculate the tilt of the lens.

Using the collected information, the three coordinates (x, y, and z) of two points were determined: the locations of the upper and bottom crosses. By drawing a straight line between these two points, a vector representing the lens tilt was obtained. Ideally, with the lens in a perfectly flat position, both points would have the same x and y coordinates, differing only in the z-coordinate, which would correspond to the distance between the centers of curvature of the biconvex lens.

The points corresponding to the upper and bottom crosses, as well as the vector representing the lens tilt, are illustrated in Figure 32. Additionally, it shows the projection of the cross formed on the lens surface (surface cross) and the side camera view of the lens. While the side camera provides a useful visualization of the lens tilt, its perspective is limited. If the tilt occurs in a direction outside the camera's field of view, direct observation may not be possible. Despite these limitations, this visualization serves as a valuable tool for estimating the lens position.

5.2 CORRECTION OF THE COORDINATE SYSTEM ORIGIN FOR THE COMMANDER 6 ACTUATOR

With the data regarding the lens positioning and positioning errors, the next step is to use the actuator to perform the necessary adjustments. However, the coordinate system used by the Commander 6 is originally centered at the base of its lower structure, not the lens. If the lens is moved without adjusting the origin of the coordinate system, the resulting motion would lead to a translational displacement of the lens center rather than a motion aligned with the tilt calculated in the previous step, which takes the lens itself as the reference.

To address this issue, it is necessary to calculate the distance between the origin of the Commander 6 coordinate system and the point designated as the origin of the lens coordinate system. The chosen point to be the new origin is located at the center of the lens surface in contact with the gripper, directly beneath the origin of the Commander 6 coordinate system. This adjustment only involves translating the point along the z-axis, simplifying the process. To determine the distance between these two points, the dimensions of the gripper, manufactured through 3D printing, were used. Figure 33 illustrates this distance, showing the real gripper with the lens on the bottom and the 3D model used for the part's fabrication, with red lines representing

the difference between the original and adjusted coordinates origin of the actuator, on the top.

Figure 33 – Distance between C6 and lens coordinates origin points.

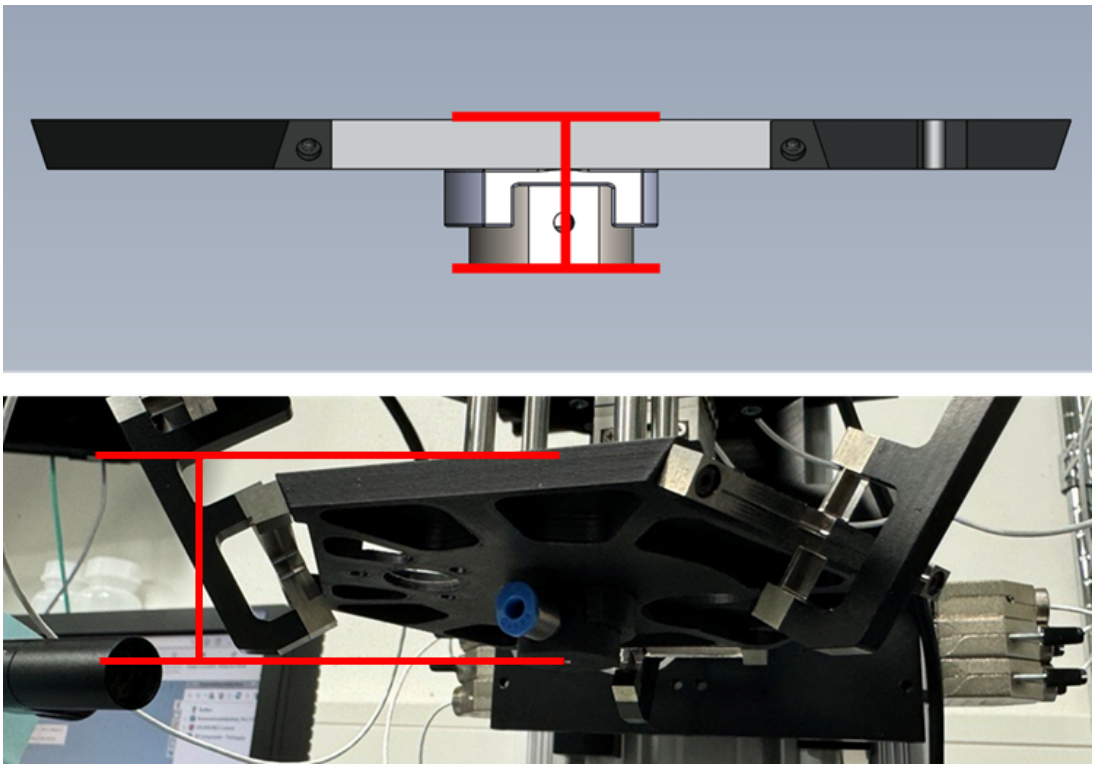

Source: Author (2024).

It is important to note that the calculated value is not perfect and contains inherent inaccuracies. As shown in Figure 34, the gripper is attached to the Commander 6 structure with the help of an adapter, also fabricated using 3D printing. Both the gripper and the adapter may not have dimensions that exactly match the original design due to limitations in the manufacturing process. Furthermore, the union between these parts introduces additional variations, as the 3D-printed surfaces are not completely smooth, making a perfect fit difficult and possibly creating slight misalignments.

Another aspect to consider is that the point chosen on the lens surface in contact with the gripper may not coincide with the path of the tilt vector shown in Figure 32. This occurs because the lens may not be perfectly positioned in the gripper, resulting in a slight displacement in the x/y plane. Despite these limitations, the inaccuracies are minor, and while they may impact the process, they do not represent a big enught obstacle to the point where additional effort to correct these errors would be justified, and that may not even be fully feasible.

Figure 34 – Lens gripper and adpter.

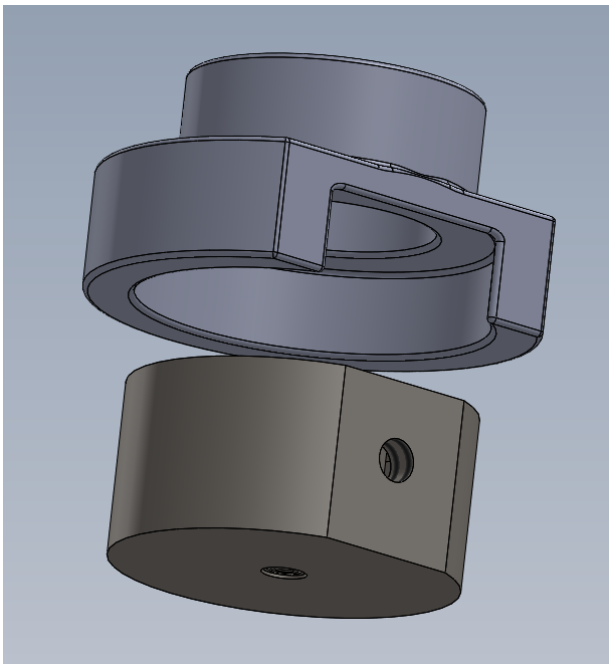

Source: Author (2024).

5.3 TIP AND TILT CORRECTION

With the data regarding the position and tilt of the lens, and the coordinate system adjusted to align with the lens, the next step is to correct the lens's tilt so that it is positioned flat. To achieve this, adjustments need to be made to the rotational coordinates Rx and Ry, that is, the lens's tilt around the x and y axes. However, due to the inaccuracies mentioned earlier, when performing this movement, the lens also undergoes a slight displacement in the x/y plane, which may result in it moving out of the autocollimator's field of view. This happens because the lens's centers of curvature can only be observed when the autocollimator's light is focused almost precisely on the point where the center of curvature is located.

Therefore, it is also necessary to adjust the x and y coordinates of the lens to ensure its visibility within the system. This positioning adjust is executed through two distinct adjustment processes: one responsible for correcting the x and y coordinates, referred to as the Field of View (FOV) adjustment process, and another dedicated to correcting the lens tilt by modifying the rotational coordinates Rx and Ry, known as the tilt adjustment process. These adjustment processes are organized hierarchically in a cascading structure. The FOV adjustment process operates at a higher level, ensuring the lens is within the system's field of view, while the tilt adjustment process functions at a lower level, correcting errors in the rotational coordinates only when the lens is properly positioned. This cascading arrangement enables continuous monitoring of the lens's position within the field of view, ensuring that tilt corrections are applied

exclusively under appropriate conditions. The overall system operation and hierarchical interaction between the two processes are illustrated schematically in Figure 35.

Figure 35 – Tip and Tilt correction system diagram.

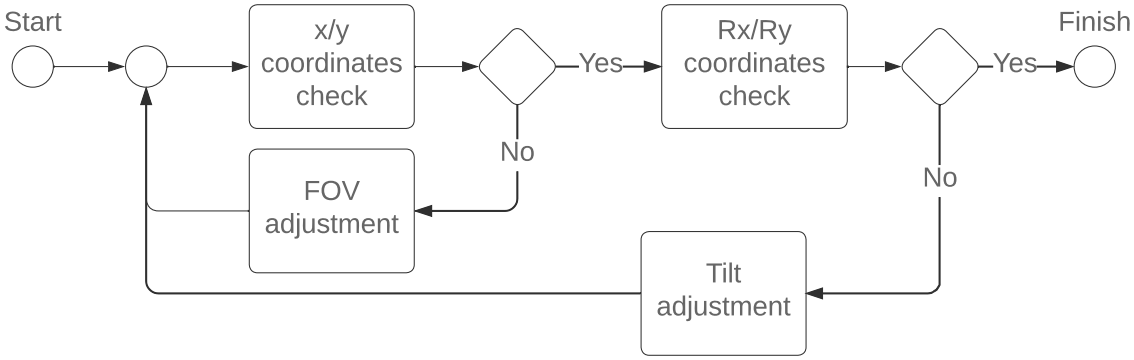

Source: Author (2024).

5.3.1 FOV adjustment process

The FOV adjustment process is responsible for moving the actuator along the x and y coordinates, ensuring that the lens remains within the field of view (FOV) of the autocollimator's camera. Figure 36 illustrates what happens when the lens exits the camera's FOV. In this case, the lens leaving the FOV was caused by adjustments to the rotational coordinates made to correct the lens's tilt without considering its positioning in the x and y coordinates. When the curvature center of the lens cannot be identified, the tilt calculation becomes impossible, preventing the continuation of the correction process for the rotational coordinates Rx and Ry.

Figure 36 – Lens moving out of the field of view.

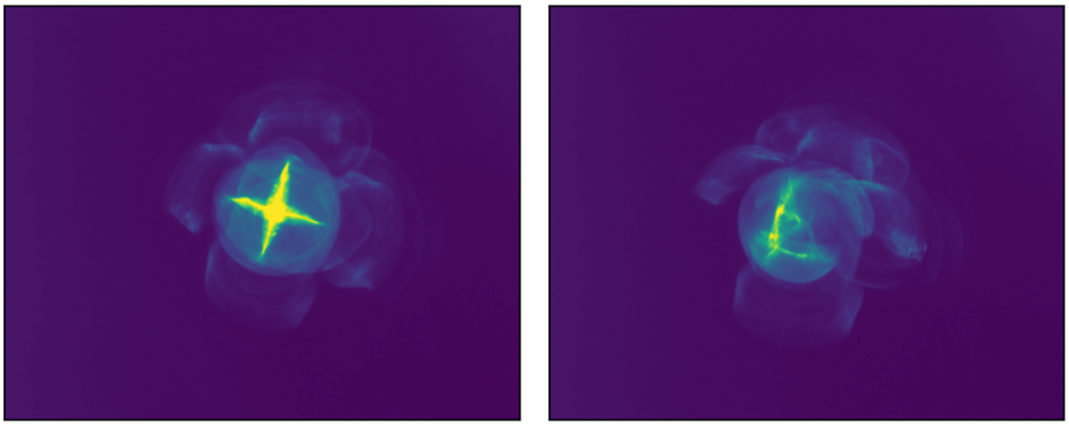

Source: Author (2024).

The adjustment process operates based on the definition of a "target", which corresponds to the desired position of the lens's center. This target is determined at the beginning of the process, when the lens is positioned in its initial position and the crosses at the lens's curvature centers are clearly visible. After each movement of the lens, the curvature centers are located again, and with this information, the center of the lens is calculated. Subsequently, it is verified whether the lens needs adjustments in the x and y coordinates. The decision to make such adjustments is based on the value of the positioning error between the current center of the lens and the target. Values to be considered or ignored are predefined and empirically tested to ensure that the lens does not exit the FOV in the subsequent iterations of the system that correct the rotational coordinates Rx and Ry.

Thus, this adjustment process is designed with hysteresis, meaning there is an error zone within which the adjustment process is not activated, preventing unnecessary adjustments caused by minor errors that do not affect the process. This approach is particularly useful in this application since the system can be affected by noise from small variations in lighting during data acquisition, which can generate insignificant errors that can be disregarded. In this way, the adjustment process becomes more efficient by avoiding corrections for errors that do not have a significant impact on the process.

Figure 37 – FOV target errors.

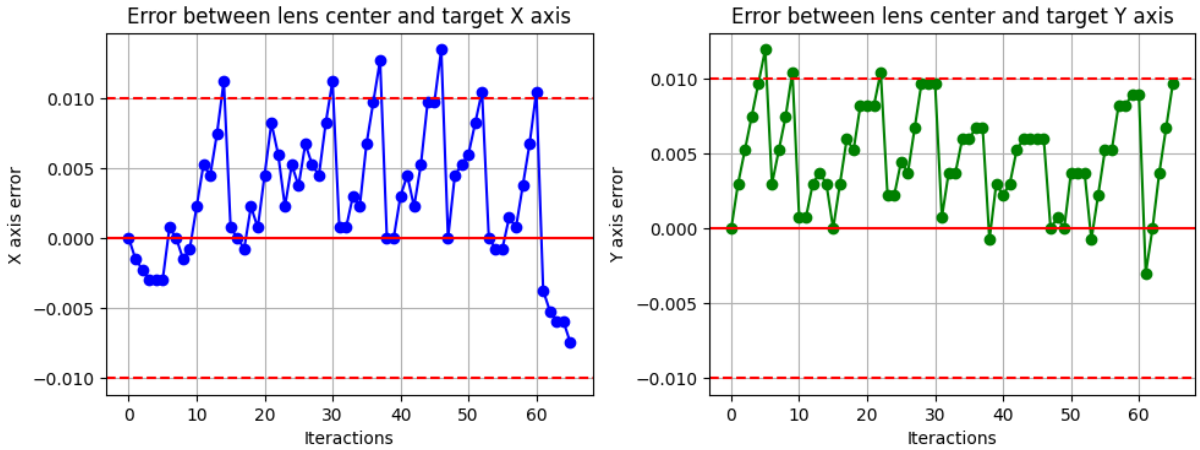

Source: Author (2024).

When the calculated error exceeds the error zone that can be disregarded, the adjustment process is activated to reposition the lens within the FOV. This is done by moving the lens along the x and y coordinates until it returns to the target position. To achieve this, the error between the current center of the lens and the target is calculated, considering the magnification of the system provided by the autocollimator's lenses, and the actuator is activated to perform the movement. Due to the coordinate

system inaccuracies, as discussed in Section 4.3.1, and lighting noise, the adjustment is not perfect, but the final error is small enough to fall within the error zone that can be ignored without compromising the process. Figure 37 illustrates the error between the center of the lens and the target at each iteration of the process. The solid red line represents the target, while the dashed red line indicates the error zone that can be disregarded. As shown, the FOV adjustment process ensures that the lens's positioning in the x and y coordinates is continuously adjusted to approach the target, ensuring that the curvature centers of the lens remain visible, allowing the tilt to be calculated, and enabling the continuation of the process to correct the lens's rotational error in Rx and Ry, with the goal of flattening the lens by the end of the process.

5.3.2 Tilt adjustment process

With the lens in position within the field of view (FOV) of the autocollimator camera and its tilt calculated, the tilt adjustment process can be activated to correct the tip and tilt errors in the Rx and Ry coordinates. However, due to the previously discussed issue, wherein adjustments to the Rx and Ry coordinates may result in the lens being displaced outside of the FOV, thereby interrupting the process, all movements in these coordinates are defined as discrete fixed steps. These steps have been empirically determined to ensure that the lens remains within the FOV. Following each movement, the FOV adjustment process is engaged to assess the lens positioning and implement any necessary adjustments. Only after this verification is the tilt adjustment process reactivated to perform the subsequent movement in the predefined fixed step.

Figure 38 – Lens tip and tilt correction.

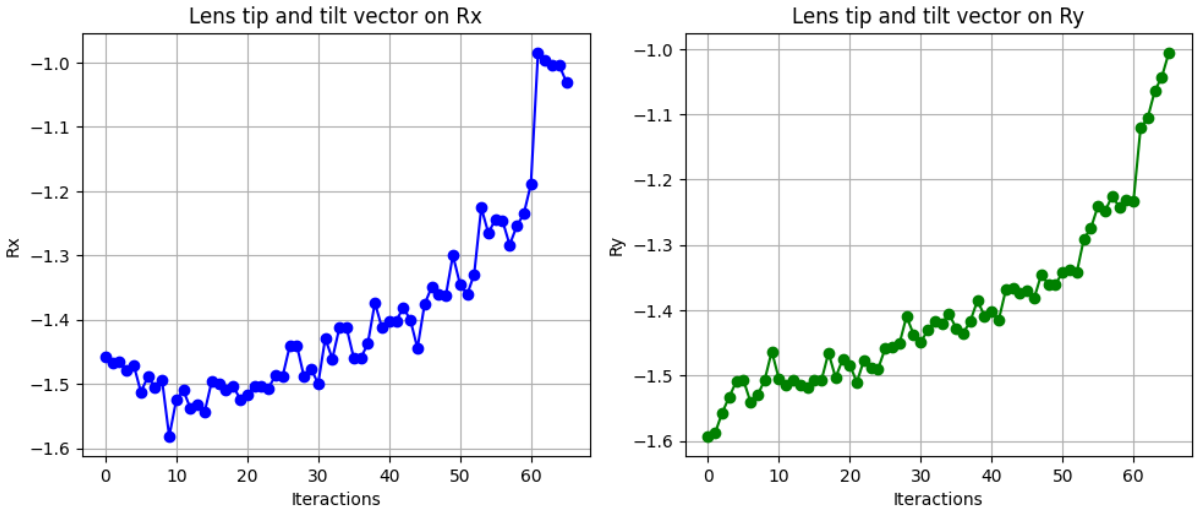

Source: Author (2024).

The Rx and Ry coordinates are corrected independently, meaning that at each iteration of the process, only one of the coordinates is adjusted. The system's deci-

sion is based on the coordinate that presents the largest error, as determined by the most recent calculation of the lens's tilt vector. It is important to note that when correcting one of the coordinates, the other is also affected due to the imprecision in the movement of the Commander 6 actuator relative to the lens's coordinate system, as previously discussed. In Figure 38, the evolution of the coordinate errors at each iteration is shown, demonstrating that the error is converging towards zero. However, due to system noise and inherent limitations, the exact value of zero is hardly reached for both of the coordinates. Considering these limitations, the system operates with an acceptable maximum error. When the error in the Rx and Ry coordinates falls below this predefined maximum error value, the system concludes its operation, considering the lens to be as flat as possible.

5.3.3 Correction Results

During the tests conducted, it was possible to minimize the issues related to the lens tilt. Figure 39 shows a side image of the lens before and after the tilt correction, indicating that the lens became flatter after the adjustment. However, after a certain point of tilt, the system is no longer able to correct the error effectively. As shown in Figure 38, the system was able to correct the tilt error of the lens up to an approximate limit of 1 degree. This limit is due to the physical capability of the actuator, which is unable to perform movements with large amplitudes. Although the tilt error is not completely corrected, the correction still manages to reduce the error without the lens moving out of the field of view (FOV), demonstrating the system's effectiveness within its operational limits.

Figure 39 – Lens before and after tip and tilt correction.

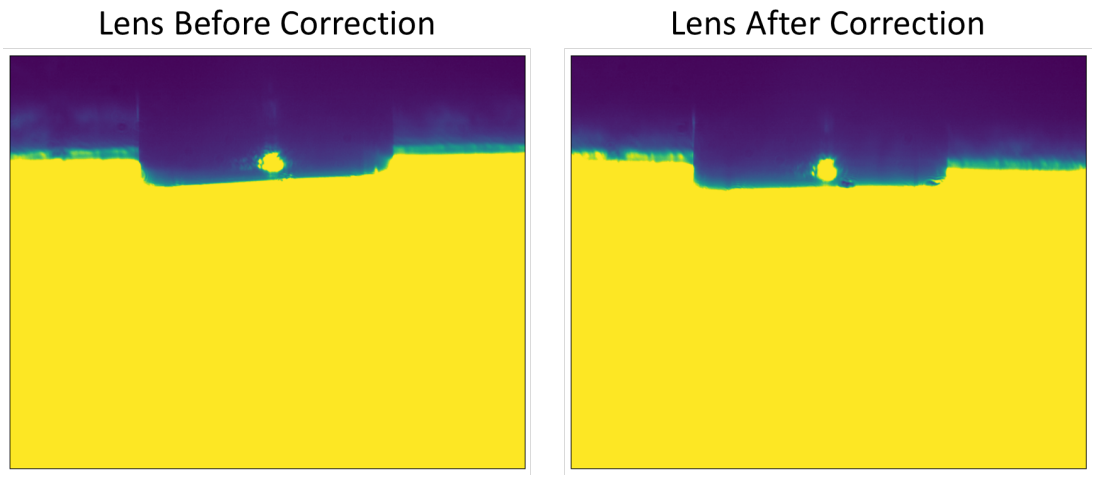

Source: Author (2024).

5.4 PROCESS EFFICIENCY ANALYSIS

To test whether the correction of the tilt actually contributes to the improvement in the alignment of the lens and the iris, the process described in Section 4 was repeated. The only change compared to the previous procedure was that the lens tilt was corrected before performing the alignment. In Figure 40 is shown a graph of the positioning error of the lens center relative to the iris center. This graph was generated using data from the side camera, in the same manner as in the previous procedure. As in the previous step, the initial positioning of the iris, when far from the center of the lens, affects the process due to the limitations of the actuator in moving the lens without causing it to leave the field of view (FOV), which can prevent the correct calculation of the curvature centers' positions.

Figure 40 – Placement error between lens and iris.

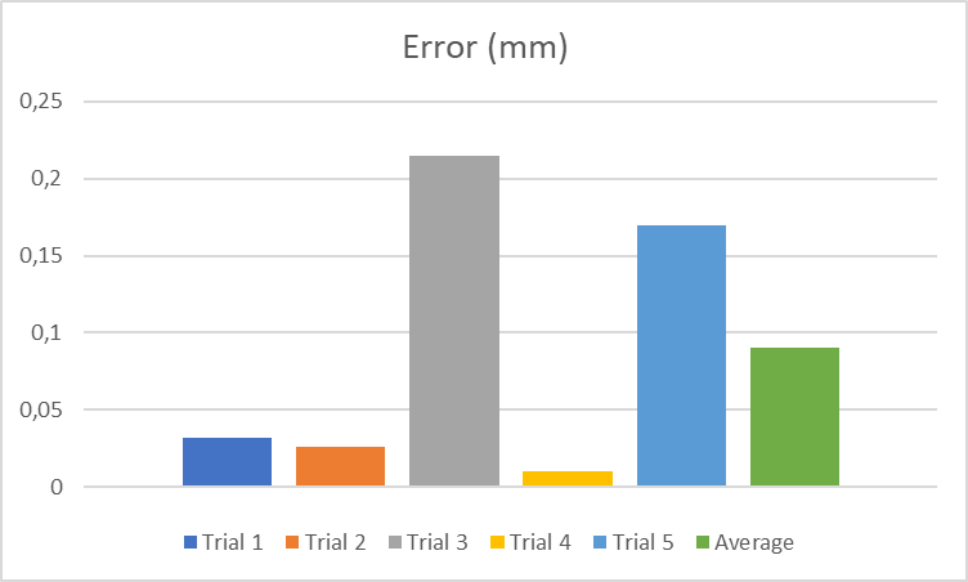

Source: Author (2024).

The lens tilt correction showed a significant reduction in the average positioning error between the lens and the iris. However, the initial positioning of the iris still has a substantial influence on the process. When the cross projected by the autocollimator light — illustrated in Figure 21, in the central image — is not close to the iris center, it becomes challenging to properly position the lens. This occurs because, when moving the lens along the x and y coordinates, it may approach the edges of the autocollimator camera's field of view (FOV), as shown in Figure 36. Under such conditions, the projected cross is not clearly captured, making it difficult to accurately calculate the center of the cross and, consequently, the center of the lens.

Correcting the lens tilt mitigates these issues, as a flat lens ensures that the cross center captured at the curvature centers has x and y coordinates closer to each

other and to the center of the FOV. As shown in the graph in Figure 41, the average positioning error decreased by almost 50% after tilt correction, highlighting the procedure's effectiveness in improving alignment.

Figure 41 – Original and improvemed process comparison.

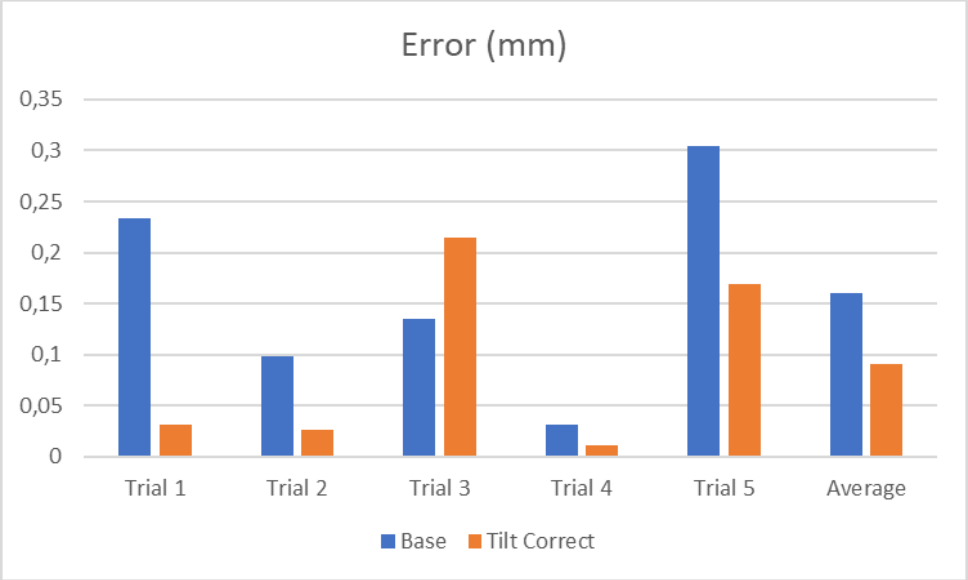

Source: Author (2024).

6 CONCLUSION

The main objective of this work was to explore the use of an autocollimator method to automate the process of constructing microlenses for an endoscope, with a focus on assessing its precision. In general, the use of the autocollimator proved suitable for obtaining appropriate images, enabling data extraction from the system and facilitating process automation. The captured images allowed for the identification of critical parameters for lens alignment, an essential step to ensure the quality and functionality of the optical system.

The data, automatically obtained by the system, was sufficient to support the automation of the lens construction process, primarily demonstrated through the alignment between the lens and the iris. A specific code was developed to assess the alignment process and automatically correct errors during the adjustment stages. This approach reduced positioning deviations by about 50%, demonstrating the efficiency of the automated system.

The developed process was able to minimize errors in alignments and microlens construction, proving to be a promising solution for automating this manufacturing stage. Although the results are positive, the work also identified opportunities for method improvement, as discussed in Section 5. These improvements could further enhance the precision and efficiency of the microlens construction process in future applications.

The improvements applied and tested focused primarily on tilt adjustment to correct the lens inclination. However, as discussed in previous sections, there remains significant room for enhancement in field of view (FOV) adjustments. Advancements in this area would enable more precise alignment of the lens with the iris, addressing the loss of accuracy observed when the curvature centers of the biconvex lens approach the limits of the FOV.

As a future improvement for the project, it would be important to enhance the precision in defining the origin point of the Commander 6 actuator's coordinate system, aligning it with the center of the lens. Aligning the actuator's x and y coordinate directions with the x and y coordinates captured by the camera, as discussed in Section 4.3.1, would also contribute to improving the precision.

Additionally, it would be interesting to explore the relationship between movements in the Rx and Ry coordinates and the effect of the autocollimator's camera in x and y coordinates. This would allow for the simultaneous correction of both rotational coordinates, making the process more efficient and minimizing the increase in error of one rotational coordinate when correcting the other, thus enabling the actuator to correct larger tilt errors.

Furthermore, applying a proportional controller to the tilt control would be beneficial. This approach would make the process more efficient by allowing larger errors to be corrected with larger, non-fixed steps, while decreasing step size as the error reduces, providing more precise control. Such adjustments could improve both the precision and efficiency of the process, as well as increase the range in which the system is capable of correcting the lens tilt.

REFERENCES

BALL, D. W. The baseline - telescope optics: Fundamental spectroscopic principles. **Spectroscopy**, v. 20, n. 1, 01 2005. ISSN 0195-6701. Disponível em: https://alfresco-static-files.s3.amazonaws.com/alfresco_images/pharma/2014/08/22/d1f456c0-f870-43bd-8c6e-293c6c6e76e0/article-142103.pdf.

BOYAT, A. K.; JOSHI, B. K. A review paper: Noise models in digital image processing. **International Journal of Engineering Research and Technology**, v. 10, n. 10, p. 1507–1510, 2021. Disponível em: https://arxiv.org/pdf/1505.03489.

GAAB, M. R. Instrumentation: Endoscopes and equipment. **World Neurosurgery**, v. 79, n. 2, Supplement, p. S14.e11–S14.e21, 2013. ISSN 1878-8750. Disponível em: https://www.sciencedirect.com/science/article/pii/S1878875012001659.

GECKELER, R. D.; JUST, A. **Angle Comparison Using an Autocollimator**. 2018.

DE GROEN, P. C. History of the endoscope [scanning our past]. **Proceedings of the IEEE**, v. 105, n. 10, p. 1987–1995, 2017.

HASHEMI, N. S.; BABAEI AGHDAM, R.; BAYAT GHIASI, A.; FATEMI, P. Template matching advances and applications in image analysis. **Journal of Imaging**, v. 6, n. 4, p. 38, 2020. Disponível em: https://arxiv.org/pdf/1610.07231.

HEINISCH, J.; DUMITRESCU, E.; KREY, S. Novel technique for measurement of centration errors of complex completely mounted multi-element objective lenses. **Proc SPIE**, v. 6288, 08 2006.

HORNBERG, A. **Handbook of Machine and Computer Vision: The Guide for Developers and Users**. 2nd, revised and updated. ed. Weinheim, Germany: Wiley-VCH, 2017. ISBN 9783527413393.

JYOTHI, S.; K.BHARGAVI. A survey on threshold based segmentation technique in image processing. **26. K. Bhargavi, S. Jyothi**, v. 3, 11 2014.

KEYES, R. Physical problems of small structures in electronics. **Proceedings of the IEEE**, v. 60, n. 9, p. 1055–1062, 1972.

KUO, C.-J. et al. Improving defect inspection quality of deep-learning network in dense beans by using hough circle transform for coffee industry. *In*: **2019 IEEE International Conference on Systems, Man and Cybernetics (SMC)**. [S.l.: s.n.], 2019. p. 798–805.

KWEON, G.; KIM, C. Aspherical lens design by using a numerical analysis. **Journal of the Korean Physical Society**, v. 51, n. 1, p. 93–103, 07 2007.

LANGEHANENBERG, P.; DUMITRESCU, E.; HEINISCH, J.; KREY, S.; RUPRECHT, A. Automated measurement of centering errors and relative surface distances for the optimized assembly of micro-optics. 02 2011.

MARTINY, H.; FLOSS, H.; ZüHLSDORF, B. The importance of cleaning for the overall results of processing endoscopes. **Journal of Hospital Infection**, v. 56, p. 16–22, 2004. ISSN 0195-6701. The 7th International BODE Hygiene Days. Disponível em: https://www.sciencedirect.com/science/article/pii/S0195670103005139.

MISHRA, V. K.; KUMAR, S.; SHUKLA, N. Image acquisition and techniques to perform image acquisition. **SAMRIDDHI: A Journal of Physical Sciences, Engineering and Technology**, SMS Journals, v. 9, n. 1, p. 21–24, 2017.

PETROU, M. M. P.; PETROU, C. **Image Processing: The Fundamentals**. Hoboken, NJ: Wiley, 2006. ISBN 9780470017660.

RUSS, J. **Image Processing Handbook**. Boca Raton, FL: CRC Press, 2007. ISBN 9780203881095.

TRIPTICS. **OptiTest: a complete range of Optical Instruments**. Wedel, Germany, 2013. Available at https://trioptics.com/wp-content/uploads/2019/09/OptiTest-EN-V009.pdf.

VERMA, R.; ALI, J. A comparative study of various types of image noise and efficient noise removal techniques. **International Journal of Advanced Research in Computer Science and Software Engineering**, v. 3, p. 617–622, 01 2013.

YUAN, J.; LONG, X. CCD-area-based autocollimator for precision small-angle measurement. **Review of Scientific Instruments**, v. 74, n. 3, p. 1362–1365, 03 2003. ISSN 0034-6748. Disponível em: https://doi.org/10.1063/1.1539896.